Review

Not peer-reviewed version

Considerations, Advances, and Challenges Associated with the Use of Specific Emitter Identification in the Security of Internet of Things Deployments: A Survey

Joshua H. Tyler , Mohamed K.M. Fadul , Donald R. Reising *

Posted Date: 18 July 2023

doi: 10.20944/preprints202307.1165.v1

Keywords: Specific Emitter Identification, Radio Frequency Fingerprinting, Physical Layer Authentication, Physical Layer Security, Internet of Things

Article

Considerations, Advances, and Challenges Associated with the Use of Specific Emitter Identification in the Security of Internet of Things Deployments: A Survey

Joshua H. Tyler [1,†], Mohamed K. M. Fadul [1,†] and Donald R. Reising [1,†,*]

[1] University of Tennessee at Chattanooga; {ygm111, lzw784}@mocs.utc.edu, donald-reising@utc.edu
* Correspondence: donald-reising@utc.edu
† These authors contributed equally to this work.

Abstract: Initially introduced almost thirty years ago for the express purpose of providing electronic warfare systems the capabilities to detect, characterize, and identify radar emitters, Specific Emitter Identification (SEI) has recently received a lot of attention within the research community as a physical layer technique for securing Internet of Things (IoT) deployments. This attention is due in large part to SEI's demonstrated success in passively and uniquely identifying wireless emitters using traditional machine learning and the success of Deep Learning (DL) within the natural language processing and computer vision areas. SEI exploits distinct and unintentional features present within an emitter's transmitted signals. The existence of these distinctive and unintentional features is attributed to slight manufacturing and assembly variations that exist within and between the components, sub-systems, and systems that comprise an emitter's Radio Frequency (RF) front end. Although sufficient to facilitate SEI, these features do not hinder normal operations such as detection, channel estimation, timing, and demodulation. However, despite the plethora of SEI publications, it has remained largely a focus of academic endeavors that primarily focus on proof-of-concept demonstration and little to no use in operational networks for various reasons. The focus of this survey is a review of SEI publications from the perspective of its use as a practical, effective, and usable IoT security mechanism, thus we use IoT requirements and constraints (e.g., wireless standard, nature of their deployment) as a lens through which each reviewed paper is analyzed. Previous surveys have not taken such an approach and have only used IoT as motivation, a setting, or a context. In this survey, we consider operating conditions, SEI threats, SEI at scale, publicly available data sets, and SEI considerations that are dictated by the fact that it is to be employed by IoT devices or IoT infrastructure.

Keywords: specific emitter identification; radio frequency fingerprinting; physical layer authentication; physical layer security; internet of things

1. Introduction

The Internet of Things (IoT) consists of two key components: (i) semi-autonomous devices that leverage inexpensive computing, networking, sensing, and actuating capabilities to sense and carry out actions within the physical world, and (ii) connection to the Internet [1]. It is important to note that our use of "IoT" encompasses the Internet of Battlefield Things (IoBT), Internet of Military Things (IoMT), Industrial IoT (IIoT), Internet of Vehicles (IoV), and other devices that satisfy the above definition. By the year 2025, the number of IoT deployments is projected to reach seventy-five billion [2–4]. Continued IoT deployments create an even larger surface over which bad actors can conduct attacks to carry out nefarious activities and exploitation of individuals or sets of IoT devices as well as their associated infrastructure. Disturbingly, a majority of IoT devices employ weak or no encryption at all [5]. The use of weak or no encryption is attributed to: (i) limited on-board computational resources (e.g., memory, power, etc.), (ii) prohibitive manufacturing costs, and (iii) scalability challenges associated with implementation and key management at scale [5–7]. Weak or the lack of encryption is being successfully exploited and abused [8–15]. In light of this information, there is a critical need for an effective means through which to secure IoT devices and their corresponding infrastructure. One solution that is being put forward is a physical layer-based approach known as Specific Emitter Identification (SEI) [16–18].

Almost thirty years ago, SEI was introduced with the purpose of providing electronic warfare systems the functionality of detecting, characterizing, and identifying radar systems via immutable features present within their transmitted signals [19–23]. The presence of these immutable features has been attributed to the components, sub-systems, and systems that comprise the radar's Radio Frequency (RF) front end. Figure 1 provides a representative illustration of the specific signal features that can be exploited by an SEI process. Based upon this visualization and the nature of the features' origins, the collection, generation, grouping, or learning of these specific features are commonly referred to as an RF fingerprint or RF-Distinct, Native, Attributes (RF-DNA) fingerprint. RF-DNA captures the essence of an emitter's identity in much the same way as a person's own DNA is essential to determining who an individual is in terms of traits, features, and so on. SEI is advantageous due to its: (i) passive nature, which means that the targeted emitter generates signals, as part of its intended mission, without external stimulation, (ii) exploitation of distinct, unique, and organic features that are unintentionally imparted to the transmitted signal by the target emitter's RF front-end components, (iii) ability to quantitatively measure the exploited features present within the signal, and (iv) exploitation of persistent features across time, location, and environments. The success of radar SEI led to it being adopted as a potential means through which to augment higher level (e.g., encryption, MAC address filtering, etc.) security mechanisms employed within private and public wireless communication networks [17,24–88].

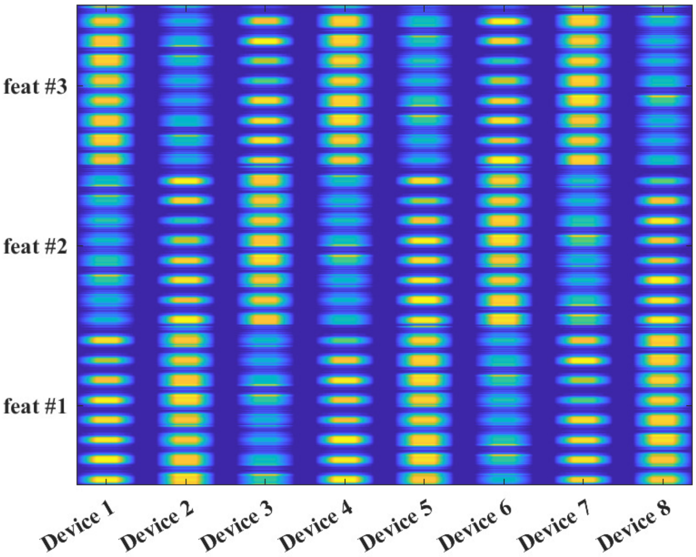

Figure 1. Representative illustration showing an average RF fingerprint for eight commercial emitters of the same manufacturer and model at a signal-to-noise ratio of 30 dB. This unique presentation has been designated RF-DNA because it highlights the "Distinct, Native, Attributes" or DNA found and exploited within an emitter's transmitted signals [34].

Despite the amount of research conducted within the SEI area, it still remains largely a focus of academic efforts with little to no use as a security mechanism within operational wireless communication deployments. This is because such deployments must contend with (i) various operating environments and conditions whose dynamic nature obscures SEI exploited signal features, (ii) emitters that may enter and leave the network, change location or service Base Station (BS)/Access Point (AP), (iii) networks that consist of hundreds to thousands of authorized emitters let alone unknown emitters that are not part of the authorized set, and (iv) user devices that are constrained in compute, memory, or other resources essential to SEI steps or the process as a whole. Additionally, little focus has been placed on the essence of SEI in terms of the origin or cause of a particular feature or features as well as how interactions within the emitter's RF front-end impact them. Lastly, SEI research predominately treats the to-be-identified emitter as a passive source that is incapable of or unwilling to actively alter its signals or signal features to reduce SEI's effectiveness or defeat it altogether. These observations and the critical need for IoT security are the impetus for this comprehensive survey of existing literature focused on chronicling recent advances that address one or more of the above observations and their pertinence to IoT security. We classify these existing works based upon the following criteria: (i) isolation of the source or sources of a feature or set of features within an emitter's RF front-end, (ii) operating conditions, (iii) processes designed to impede or thwart SEI, (iv) SEI at scale, (v) size and availability of signal databases, and (v) IoT imposed resource limitations or considerations.

A comparison between the topics addressed in this paper and those of prior, related survey papers are provided in Table 1. The authors of [89] survey physical fingerprinting techniques for the identification of mobile phones, including SEI works as well as other mobile phone components including but not limited to the camera, microphone, and display. Their survey also considers Medium Access Control (MAC) layer approaches in addition to Physical (PHY) layer approaches that include RF fingerprinting. One key contribution of the survey in [89] is the adoption of four fingerprint requirements borrowed from the biometrics domain [90]. These requirements are:

1. *Universality:* Every emitter possesses the characteristics or features used to identify it.
2. *Uniqueness:* No two emitters have the exact same RF fingerprint or SEI exploited features.
3. *Permanence:* The RF fingerprint features are invariant to time or environmental conditions.
4. *Collectability:* The exploited features can be quantitatively measured.

and are included here because they remain pertinent and in some cases unaddressed, thus they inform our observations, and analyses presented herein. While the authors of [91] survey Physical Layer Authentication (PLA), which encompasses SEI as well as channel-based authentication schemes that take advantage of Jakes uniform scattering model to identify two communicating devices based on the unique channel response that exists between them [92]. Thus, the survey in [91] provides limited coverage of SEI, in particular, the authors note Deep Learning (DL) is an emerging PLA technique, the threat of SEI impersonation based on the work in [93], and IoT as the "next wave of technological evolution", which differs from our IoT-centric SEI survey. The authors of [94] focus on surveying SEI works based on the signal portions from which RF fingerprints are extracted with the majority covering transient-based SEI. The authors of the survey in [95] also focus on PLA, thus SEI only accounts for a small portion of the works surveyed. The SEI works covered in [95] are analyzed based on the signal region from which SEI features are extracted, the features used for SEI, and the classification processes. The survey presented in [96] covers the various machine-learning approaches used to detect and identify IoT devices. However, since the scope of the survey is on machine-learning approaches means that SEI as well as other IoT device detection and identification works are included. The survey presented by the authors of [97] focuses on physical layer security in fifth-generation (5G) wireless IoT networks and primarily focuses on defining security threats and their purpose, categorizing the threats, and surveying 5G-specific countermeasures. The authors of [97] do mention SEI as a physical layer security approach for authenticating legitimate IoT devices but do not survey SEI itself, which we do.

Table 1. Comparison of the content of this paper versus previous survey papers within the RF fingerprinting area.

	Survey								
	This paper	[89]	[97]	[91]	[94]	[95]	[98]	[99]	[96]
Year	2023	2017	2019	2020	2020	2021	2022	2022	2022
IoT Motivated	✓		✓	✓		✓	✓	✓	✓
Handcrafted SEI	✓	✓		✓	✓	✓	✓	✓	✓
DL-based SEI	✓	✓		✓		✓	✓	✓	✓
Operating Conditions	✓	✓							
Threats to SEI	✓			✓					
SEI at scale	✓								
IoT Limitations	✓		✓						

Our survey differs from those presented by the authors of [95,96,98,99] that use IoT as motivation or context for their surveys but do not use IoT as a lens through which to analyze the surveyed SEI papers as we do herein.

The remainder of this paper is as follows. Section 2 describes what SEI is, the signal regions from which it can be learned or extracted, an equation expressing SEI feature variation within a signal, and SEI approaches that leverage features associated with specific RF front-end components; Section 3 summarizes works that address the performance of SEI under alternate operating channel (a.k.a., non-Gaussian noise) and temperature conditions; Section 4 surveys papers that specifically look into adversaries focused on defeating or inhibiting SEI; Section 5 looks into performing SEI in large IoT deployments and across signal collections; Section 6 surveys publicly available signal data sets that can be used for SEI; Section 7 covers paper that develop SEI approaches under the consideration of IoT imposed constraints (e.g., limited memory) and receiver-agnostic SEI to allow every receiver within an IoT deployment to be used by an SEI process; Section 8 covers challenges facing IoT-focused SEI that are not covered in the previous sections because there are too few papers to warrant individual sections; and Section 9 concludes the paper.

2. The Essence of Specific Emitter Identification

SEI approaches can be assigned to two general categories, which are designated here as (i) constellation-based and (ii) signal-based. Constellation-based SEI approaches extract discriminatory, emitter features (e.g., phase and amplitude shifts from the ideal point) from the individual point, collection of points, or distributions associated with the employed digital modulation scheme's two-dimensional, complex plane scatter diagram [93,100–102]. A digital modulation scheme's constellation is a byproduct of the demodulation process and its corresponding points are generated by sampling each signal symbol at a specific time. The key to constellation-based SEI is that it requires the completion of part or all of the demodulation process.

In signal-based SEI, discriminatory emitter features are extracted from the signal's discrete-time samples or their representation (e.g., spectrum). signal-based SEI can be further subdivided into transient and steady-state-based approaches. Figure 2 illustrates the transient and steady-state portions of an IEEE 802.11a Wireless-Fidelity (Wi-Fi) signal. In transient-based approaches, SEI is performed by extracting discriminating features from the temporary transitions that exist at the beginning and end of a transmission [32,103–105]. These turn-on and turn-off transients are very short in duration, thus requiring high sampling rates in the gigabytes range [106] and making them difficult to detect and exploit for SEI as the channel conditions degrade (i.e., lower signal-to-noise ratios) [94,107].

Due to the limitations associated with transient-based approaches, other SEI works have focused on extracting the discriminatory features from the steady-state portion of the signal. The steady-state portion is longer in duration and of higher energy than that of the transient, thus making its detection much easier. Signal-based SEI approaches can exploit a known, fixed sequence of signal symbols (e.g., the IEEE 802.11a Wi-Fi preamble) [42], the information carrying symbols (i.e., the signal's payload) [58], or a combination of the two.

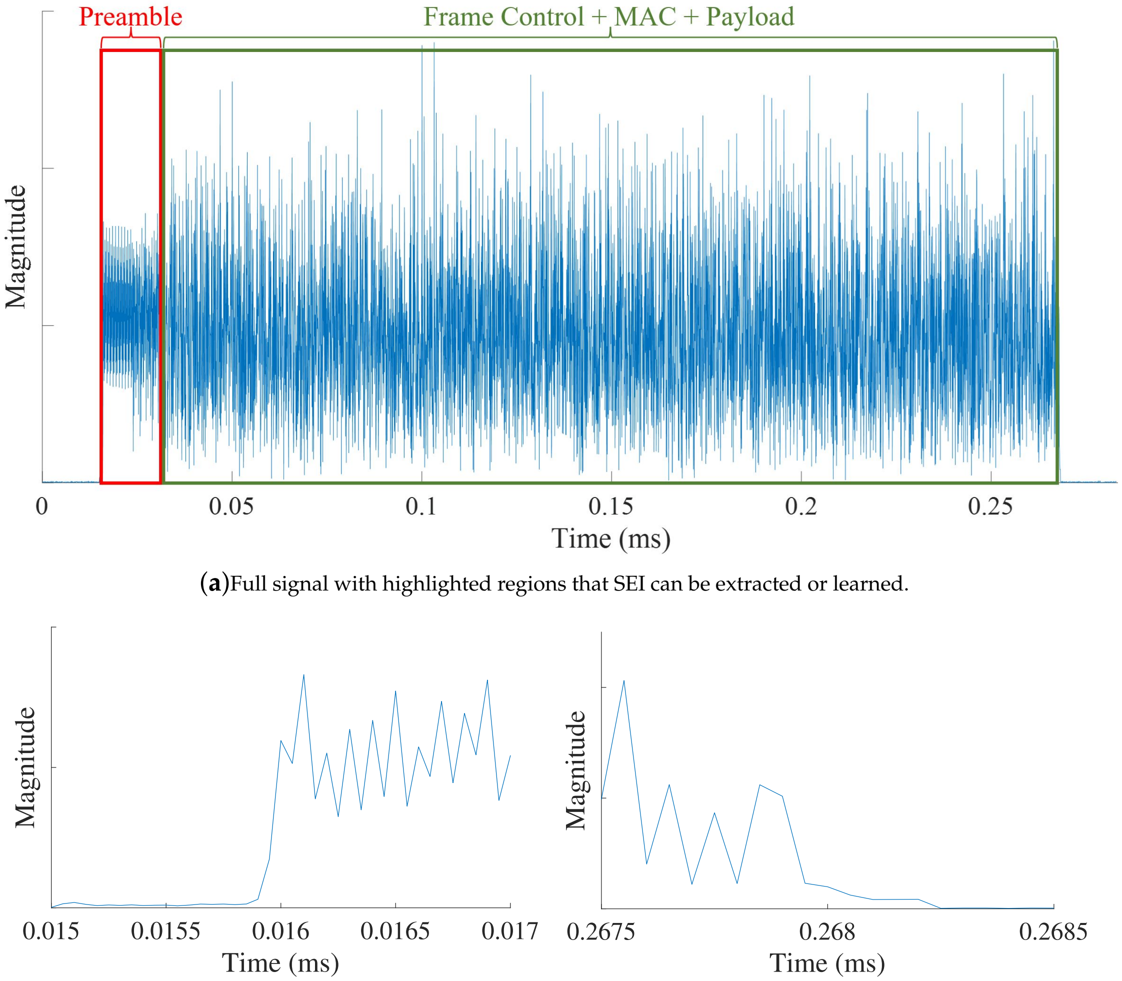

(**a**)Full signal with highlighted regions that SEI can be extracted or learned.

(**b**)Turn-on transient

(**c**)Turn-off transient.

Figure 2. Representative illustration showing the: (a) full signal, (b) turn-on transient, and (c) turn-off transient portions of a transmitted signal from which signal-based SEI features can be extracted or learned.

Regardless of the signal portion from which SEI features are extracted, the exploited features are often expressed as variations from the ideal signal's values. Specifically, variations in an ideal signal's amplitude, phase, and frequency, which is mathematically given as,

$$r(t) = A(t)[1 + \Delta A(t)] \exp\{j[2\pi(f_0 + \Delta f)t + \phi_0 + \phi(t) + \Delta\phi(t)]\} + n(t), \; 0 \le t \le T, \tag{1}$$

where $A(t)$ is intentional amplitude modulation, $\Delta A(t)$ is unintentional amplitude modulation, ϕ_0 is the initial phase, f_0 is the carrier frequency, Δf is the Carrier Frequency Offset (CFO), $\phi(t)$ is intentional phase modulation, $\Delta\phi(t)$ is unintentional phase modulation, $n(t)$ is channel noise, and T is the total duration of the signal [108,109]. It is the unintentional features that are exploited by SEI.

Researchers have conducted investigations into specific RF front-end components' contributions and impacts on SEI performance based on Equation (1). These investigations considered the role of the RF front end's power amplifier, Analog-to-Digital Converter (ADC), Local Oscillator (LO) [49,110–112], and baseband Low-Pass Filter (LPF) [113,114].

The authors of [49] assess the impact of CFO on the SEI process using four Cisco AIR-CB21G-A-K9 COTS emitters. The experiments show how SEI performance is impacted when CFO is and is not present as well as when each emitter's CFO distribution is unique of CFO is unique. The authors use Gabor Transform (GT) derived RF-DNA fingerprints and a Multiple Discriminant Analysis/Maximum Likelihood (MDA/ML) classifier. The results show that the identification of individual emitters is higher when CFO is present versus when it is not present. The authors also show that SEI performance is highest when each emitter's CFO distribution is unique (a.k.a., non-overlapping with the distributions of all other, known emitters). When each emitter's CFO distribution was modified to match Emitter #4's distribution, SEI performance is similar to when the CFO of all emitters is removed. When the CFO for each emitter is randomly drawn from the same distribution, SEI performance is consistent with the case when the CFO is removed. The results in [49] show that SEI performance improves when CFO is present and uniquely distributed across each emitter.

The authors of [110] improve SEI performance by introducing a technique called the passive RAdiometric Device Identification System (PARADIS). PARADIS uses an emitter's (i) frequency error (a.k.a., CFO), (ii) SYNC correlation, (iii) In-phase & Quadrature (IQ) offset (a.k.a., DC offset), (iv) magnitude error, and (v) phase error. The SYNC correlation is calculated by correlating the received signal with an ideally generated one. The magnitude error is calculated by calculating the absolute distance between the signal's payload constellation point and the ideal constellation point location. The phase error is calculated as the difference in phase between the received and ideal constellations. The authors assess performance when using either a Support Vector Machine (SVM) or a k-Nearest Neighbors (kNN) classifier. The authors use the following performance metrics to compare the two networks: (i) average error rate, (ii) False Accept Rate (FAR), (ii) False Reject Rate (FRR), and (iv) worst-case similarity. The average error rate is the average misclassification rate calculated across all emitters in the set. An emitter's FAR is the average rate at which the classifier incorrectly assigns a different emitter's signal to that emitter (i.e., Emitter A's FAR is the rate at which Emitter B is called Emitter A). An emitter's FRR is the average rate at which the classifier wrongly assigns the emitter to another emitter (i.e., Emitter A's FRR is the rate at which Emitter A is called Emitter B). The worst-case similarity is the highest rate at which an emitter is falsely assigned another emitter's features (i.e. if Emitter B is called Emitter A more than Emitter C is called Emitter A, the worst-case similarity reports the rate at which Emitter B is called Emitter A). The experiment uses one hundred and thirty-eight ORBIT nodes that communicate using Atheros Network Interface Controllers (NIC) transmitting at 2.412 GHz and communicating via the IEEE 802.11b Wi-Fi. Using the SVM classifier, the highest FRR is 10%, and the highest worst-case similarity rate is 16%. These rates increase when using the kNN, where the highest FRR increases to 62% and the worst-case similarity increases to 40%.

The authors of [111] propose comparing an estimated CFO value to the actual, received CFO to either grant or deny network access to an emitter. For an emitter to be granted access, it must fall within a given tolerance around the signal's CFO. Two factors determine this tolerance: (i) Doppler shift and (ii) receiver-incident Signal-to-Noise Ratio (SNR). The authors role-play a threat model where Alice is the true, trusted emitter, Eve is the adversary attempting to gain access to the network, and Bob is the authenticator that grants network access. Both Alice and Eve are modeled using the same Software Radio Peripheral (USRP) Software-Defined Radio (SDR). The authors' experiment is conducted using the preambles extracted from IEEE 802.11a Wi-Fi frames transmitted at a carrier frequency of 2.5 Ghz. At SNR values above 10 dB, Bob successfully rejects Eve at a rate greater than 80%.

The authors of [113] introduce a method of validating the identities of trusted emitters through the use of IQ Imbalance (IQI). IQI is defined as the difference between the ideal, modulated constellation points and the real, received constellation points. This is similar to the method introduced by the authors of [111]. The authors of [113] track IQI per emitter and assign a Gaussian distribution to account for perturbations caused by the wireless channel. The received signal's IQI is calculated and mapped to the known IQI, and the received signal is assigned to the emitter whose distribution resulted in the highest likelihood value using the mapped IQI value. In the simulation, Bob can correctly authenticate Alice's identity at a rate of over 98% at an SNR of 18 dB and higher.

3. Specific Emitter Identification Operating Conditions

IoT devices operate in various environments, thus effective SEI processes must contend with environmental and environment-induced effects that impact the channel or the emitter being identified. This section reviews SEI publications focused on operating channel conditions and emitter operating temperatures.

3.1. Operating Channel Conditions

Despite the amount of research within the SEI space most of it has been conducted using simulated channel conditions and a preponderance of those assume an Additive White Gaussian Noise (AWGN) channel model. Thus, this section reviews SEI works that employ alternate channel models with the intent of moving SEI from a proof-of-concept demonstration to a realistic IoT security approach.

In [58,63,115–119], SEI performance is assessed using a multipath channel, but the specific characteristics of the multipath channel are unknown, unstated, or not disclosed.

The authors of [120] propose a semi-supervised SEI approach built upon a Triple-GAN network. First, a representation network extracts features–from the received RF signals–that are used to train the Triple-GAN network, and feedback learning is used to assist the representation network in learning more discriminative features. Similarly, the authors of [121] present an unsupervised-learning SEI approach that uses an Information maximized Generative Adversarial Network (InfoGAN) to train a discriminative model for emitter identification. The authors of [121] also apply RF Fingerprint Embedding (RFFE) by computing the bispectrum histogram from the received signal and integrating the resulting features into the InfoGAN's training process. The efforts in [120,121] evaluate SEI performance within a multipath environment that is modeled using a Nakagami-m distribution. Although the value of the distribution shape parameter m is chosen to simulate Rayleigh and Rician fading channels, the multipath fading channel is not described in detail. For instance, the authors in [120,121] do not specify critical channel configuration details such as the number of reflectors or paths and delay spread values. This information is important when assessing and analyzing SEI performance for different channel lengths representing various multipath environments.

In [122], the authors present a DL-based device fingerprinting approach that leverages Multiple-Input Multiple-Output (MIMO) system capabilities and Space-Time Block Codes (STBCs) to mitigate the adverse effects AWGN and Rayleigh fading channels have on SEI performance. Since SEI features are distorted by Rayleigh fading channels, the approach in [122] exploits the MIMO system's multiple received signal streams to reconstruct a less-distorted version of transmitted signals, which are later used for model training and classification. Without knowledge of the channel state information, the transmitted signal is estimated at the receiver using two blind-source-separation and blind-channel-estimation algorithms neither of which rely upon the use of pilot symbol-based estimation. The first algorithm fully calculates the channel matrix by using Orthogonal STBC (OSTBC) properties as well as the received signal covariance matrix. The second algorithm attempts to partially estimate the channel by calculating a solution to a subset of the channel matrix up to some ambiguity. The receiver's reconstructed signals are expected to exhibit channel-immune characteristics when using DL models trained for channel conditions that differ from those present in the received signals before reconstruction. The presented approach's SEI performance is evaluated by adjusting the emitters' phase noise, CFO, and IQ gain imbalance hardware impairments within a fixed range. This allows the authors of [122] to simulate up to ten emitters that each have three antennas and communication via Wi-Fi. The approach is also tested for a varying Average Path Gain (APG) and Doppler shift and emitter identification performed using a Convolutional Neural Network (CNN). The authors leverage MIMO technology to mitigate channel effect variation on SEI performance. MIMO results in a 30%

improvement in identification accuracy for AWGN channels and a minimum of 50% improvement for Rayleigh channels.

The authors of [123] propose an SEI approach that exploits the different spectrum of adjacent signal symbols, known as the Difference of the Logarithm of the Spectrum (DoLoS), to extract RF Fingerprint (RFF) features that are robust to time-varying channels. The approach in [123] is motivated by the fact that during coherence time, the channel is considered stationary; therefore, two different symbols in one packet exhibit different SEI features but have the same channel response. DoLoS is calculated for two different symbols of the same received signal to extract SEI features that are independent of time-varying channel effects. The proposed approach is evaluated using IEEE 802.11n signals collected from seven emitters located at twelve different locations to simulate different channel conditions. DoLoS is used to calculate the spectrum difference between the IEEE 802.11 Wi-Fi preamble's Short Training Symbol (STS) and Long Training Symbol (LTS) sequences. The resulting DoLoS response is used to train and evaluate a CNN-based SEI process. The characteristic of the assumed time-varying multipath channel including channel length, and delay spread are not described by the authors of [123]. The proposed SEI approach is evaluated using seven IEEE 802.11 Wi-Fi devices, twelve data collection positions, and two different environments. The presented SEI process achieves a maximum identification accuracy of 99.02% in the single-environment evaluation and 97.05% in the cross-environment evaluation.

The authors of [124] propose an SEI approach for wireless Orthogonal Frequency-Division Multiplexing (OFDM) device identification in time-varying channels. Their approach attempts to cancel the time-varying multipath channel effects by extracting SEI features from the emitter's non-linearity and IQ imbalance based on a Hammerstein system parameter separation technique. The algorithms in [124] are performed in three steps: (i) the Hammerstein system parameter separation technique estimates the emitter's non-linear model parameters as well as the multipath channel's Finite Impulse Response (FIR), (ii) the estimated FIR is used to obtain the best IQ imbalance parameter combination, and 3) *k*NN is used to classify the estimated non-linear model and IQ imbalance parameters obtained in the first two steps. IQ imbalance and Power Amplifier (PA) non-linearity values are set to simulate five emitters with minor differences. The proposed approach is evaluated within A Rayleigh fading channel with a maximum channel delay of nine samples. The authors of [124] do not specify the length of the Rayleigh channel or the delay spread corresponding to each path. The experimental results show that the extracted SEI features are stable and the proposed authentication method is feasible.

The authors of [125] present an SEI approach that exploits the IoT devices' PA non-linearity to generate environment-robust RFFs with the goal of improving SEI performance when signals are collected in the presence of time-varying multipath channels. The approach calculates the PA non-linearity quotient by performing element-wise division of the frequency response of two consecutive signals transmitted at two different power levels. This process mitigates the effect of the multipath channel and the resulting quotients are used to train a CNN-based classification model. The authors use transfer learning to integrate RFFs from different wireless environments to further enhance SEI performance in the presence of multipath fast fading and Doppler. First, a base model is trained using channel effect-free RFFs from signals collected in an anechoic chamber. Then, the model is retrained using samples collected from indoor or outdoor environments to emulate moderate or severe multipath fading effects, respectively. A detailed description of the multipath channel including the model type is not provided by the authors of [125]. Compared to conventional DL and spectrogram-based models, the proposed PA non-linearity quotient and transfer learning-based SEI approach improves indoor and outdoor environment performance by 33.3% and 34.5%, respectively.

The authors of [51,126] propose a channel estimator built using the Nelder-Mead (N-M) simplex algorithm to restore the SEI features prior to emitter identification when IoT signals are propagating in a multipath fading environment characterized by a Rayleigh fading model. The N-M estimator estimates the Rayleigh channel impulse response which is later used by a Minimum Mean Squared Error (MMSE) equalizer to mitigate the multipath effects on the received signals. In [126], RFFs are generated from the equalized signals by computing the GT coefficients, subdividing the normalized, magnitude of the GT coefficients into patches, and computing the statistics of variance, skewness, and kurtosis. The generated fingerprints are then used to train an MDA/ML classifier. The work in [126] analyzes the resulting SEI process using Rayleigh fading channels consisting of two, three, and five paths where the coefficient associated with each path changes for each IEEE 802.11a Wi-Fi frame. Further, [126] analyzes the effect of the Gabor patch size on the SEI classification performance. The authors of [53] present a DL-based SEI approach that uses N-M-based channel estimation and MMSE equalization, and CNN pre-training to improve SEI performance in IEEE 802.11a Wi-Fi indoor Rayleigh fading channels. The work in [53] performs SEI using Rayleigh channels comprised of up to seven paths. Further, the authors of [53] investigate different IEEE 802.11a preamble representations including a one-dimensional IQ representation and a two-dimensional time-frequency image generated from the GT coefficients. To reduce the CNN's size, augment the training data set, and improve the CNN's capability to extract shift-invariant SEI features, the authors of [53] adopt data partitioning that slices the preambles' one-dimensional and two-dimensional representations into shorter sequences and sub-images, respectively. Finally, the authors of [53] use a Convolutional AutoEncoder (CAE) to pre-train the CNN with the goal of improving both model convergence as well as SEI performance. When compared to traditional feature-engineered SEI methods, the experimental results in [53] demonstrate that using N-M channel estimation and equalization with a CAE-initialized CNN and data partitioning improves SEI identification performance by 9% at an SNR of 9 dB.

The authors of [127] present two semi-supervised learning-based approaches to restore (a.k.a., correct) SEI features when IoT signals are corrupted by Rayleigh fading channels. The first approach aims at estimating a generative function that compensates for multipath channel effects by training a Conditional GAN (CGAN) network using: (i) signals that have been corrupted by multipath channels, (ii) the originally transmitted signals without multipath, as well as (iii) the label associated with each signal. Combining the label with the signal's representation enables the CGAN's generative model to compensate for the multipath effects while preserving emitter-specific SEI features. A separate CNN model is trained to classify the CGAN corrected (a.k.a., equalized) signals. The received multipath signal is combined with all possible labels at the generator's input, and the signal is assigned to the label that achieves the highest confidence score at the output of the CNN classifier. The second approach uses a Joint CAE and CNN (JCAECNN) architecture comprised of multiple decoder heads and a single classification head to compensate for multipath effects while preserving SEI discriminating features. The JCAECNN's multiple decoder and classification heads are jointly trained such that they are capable of decomposing a multipath corrupted received signal into its original delayed and weighted versions. Each one of the delayed and weighted versions is classified separately using a CNN model and a final decision is made by combining all decisions using a highest-vote scheme. Inspired by the fact that the Rayleigh channel's path coefficients decay exponentially, the authors of [127] introduced exponentially decaying loss weights that improve the overall SEI performance. The CGAN and JCAECNN-based SEI approaches improve SEI performance by 10% when extracting emitter-specific features from signals collected under a Rayleigh fading channel comprised of five paths or reflections, which is superior to prior SEI approaches.

The authors of [128] present Channel Robust Representation Networks (ChaRRNets) for SEI when signals are received under multipath conditions. In particular, the authors build a CNN whose convolutional layers are equivariant and invariant to the channel's frequency response to mitigate or eliminate adverse multipath channel effects on the SEI process. The authors create these equivariant and invariant CNN layers by using the Albein Lie group representation of the complex-valued signals (a.k.a., the IQ samples). Their aim is to develop a CNN that can handle cases in which it is trained using signals collected under Rayleigh fading and tested using signals collected under Rician fading conditions. The authors assess ChaRRNets using signals that have simulated SEI features applied to them using an Infinite Impulse Response (IIR) filter as well as signals transmitted by real-world emitters. It is unclear the specific features that are imparted by the IIR filter; however, the SEI features do seem to be unique for each emitter and are unchanged across each emitter's simulated signals. Although such an approach is good for the validation of ChaRRNets; it is not indicative of real-world emitters whose SEI features change from one signal to another as shown by the work presented in [49]. The real-world signals used to test ChaRRNets are collected on a different day than those used for training to ensure different channel conditions. Additionally, the manufacturer and model of the real-world emitters are not provided, which makes it unclear if this is SEI at the serial number, model, or manufacturer level. The first is the most challenging case of SEI and the last is the easiest. The authors also perform "CFO augmentation" but do not explain what it is, how it performs, or a citation describing it. Unfortunately, CFO has been shown to bias DL-based SEI approaches that make them susceptible to attack [49,109,129]. ChaRRNets does outperform a conventional complex-valued CNN with an average classification performance of 65.5% versus 25.6% when training ChaRRNets using both days of real-world, "in the wild" collected signals. The authors do not present classification performance for each emitter.

3.2. *Operating Temperature Conditions*

IoT devices operate in a variety of environments, many of which impact device operating temperature. A particular example is IIoT devices that are and can be deployed in manufacturing settings associated with extreme temperatures due to the manufacturing processes themselves (e.g., steel production and processing) or the conditions under which a manufacturing process is running (e.g., non-temperature controlled building). Therefore, SEI processes must continue to provide effective and accurate emitter identification regardless of the temperature(s) under which the emitter(s) operate. The SEI publications surveyed under this section focused on the environmental temperature impacts on SEI and not emitter-connected operating temperature(s). The former is not new to the SEI community [130] but it has not received a lot of attention [106,131,132]. The latter is addressed in Section 8.5 of this survey.

The Temperature-aware Radio Frequency Fingerprinting (TeRFF) approach is presented by the authors of [106]. TeRFF uses receiver-measured CFO to discriminate one emitter from another and is motivated by the fact that this LO-dependent feature is directly influenced by the temperature of the RF front end [133]. The authors of [106] address this temperature-dependency by training a naïve Bayes classifier for each of the eight, discrete temperatures within the range of 26°C to 33°C (i.e., there is 1°C difference between consecutive temperature values). The authors adopt this approach assuming that temperature-independent SEI features are difficult to learn. An emitter's CFO value is estimated whenever that emitter operates outside the designated temperature range. To eliminate the need to compare every signal or RFF with each of the eight naïve Bayes classifier (i.e., one for each temperature), the authors of [106] require each emitter to transmit its current operating temperature via Internet Control Message Protocol (ICMP). This provides an opportunity for exploitation by nefarious actors because it provides information (a.k.a., operating temperature) about the IoT device. Additionally, the ICMP requirement adds complexity to the SEI process at the loss of its passive nature, assumes the capability is organic to the emitter or device, as well as consumes more onboard resources while increasing processing times. The last two are essential factors to consider if the TeRFF approach is deployed in IoT or IIoT deployments because they may require the integration of additional functionality or modification of the device that can limit the associated IoT devices' operational longevity. Lastly, TeRFF uses CFO as the emitter-specific feature which is an easily manipulated feature that can be exploited by nefarious actors [49].

In [132], the authors collect signals from emitters operating at temperatures of -5°C, 10°C, 25°C, and 40°C. SEI is performed using the CNN architectures of ResNet50 and InceptionV3 which learn emitter-specific features from their signals' transient region detected using a unique technique the authors coined the "double sliding window method." When CNN training and testing are performed using transients extracted from signals collected at a single temperature, the SEI performance is high. However, when the temperature of the training set of transients is different than those comprising the testing set (a.k.a., cross-temperature SEI), then SEI performance is seriously degraded. To address this performance degradation, the authors construct "blended" training and testing data sets that each contains an equal number of transients collected at each of the four temperatures. Despite this, SEI performance remains low when using the "blended" data sets with an average percent correct accuracy of 45% and 52% when the InceptionV3 and ResNet50 classifiers are used to identify emitters operating at -5°C, respectively. This represents the lowest average classification accuracy using the "blended" data set.

The authors of [134] investigate environmental temperature impacts on preamble-based SEI for temperatures ranging from -40°C to 80°C. The authors collect preambles transmitted by four HackRF One SDR emitters placed inside an environmental chamber. The emitters transmit an ideally generated IEEE 802.11a Wi-Fi frame at a carrier frequency of 2.45 GHz over a wire to a receiving USRP B210 that samples the received signals at a frequency of 40 MHz. The B210 is placed outside of the environmental chamber. Collections are performed at the previously stated temperature range in steps of 10°C for a total of thirteen different environmental temperatures. A total of 1,000 preambles are collected from each emitter at each of the designated temperatures. The authors employ four SEI approaches: (i) MDA/ML, (ii) Principal Component Analysis (PCA)/k-Means, (iii) CNN, and (iv) LSTM. The MDA/ML and PCA/k-Means approaches use GT-derived RFFs, the CNN uses the raw image of the GT normalized magnitude, and the LSTM uses the magnitude and phase of the preamble's IQ samples. When training and testing each network at ambient (a.k.a., 20°C), the MDA/ML network has an average classification accuracy across all devices of greater than 98%, the PCA/k-Means has an accuracy of 25%, and the CNN and LSTM have an average accuracy of over 90%. When classifying temperatures below and above ambient, the average classification performance decreased. The authors then trained each network on a thirteen-chose-two combination of environmental temperatures for a total of seventy-eight combinations. The results show that the highest average classification performance across all temperatures is achieved when the networks are trained on the extremes of the temperature ranges (e.g., the highest-performing LSTM network was trained at -30°C and 70°C). The results also show that blind SEI performance is higher at sub-ambient temperatures than at temperatures above ambient. The authors conclude: (i) the SEI approaches are able to generalize the emitter's RFFs better when they are given the extremes of the temperature range, and (ii) the emitter's RF front end performs more consistently at sub-ambient temperatures.

In addition to the challenge described in Section 8.5, the papers surveyed in this section show that an emitter's operating temperature remains an open problem in need of further investigation and solution development to ensure viable SEI-based security within IoT deployments.

4. Threats to Specific Emitter Identification

As with any security approach, one must remain aware of the fact that adversaries will endeavor to find ways to circumvent it. This is no different for SEI-based security approaches, thus this section provides a summary of published SEI works that investigate weaknesses or specific techniques that can be exploited by adversaries for the purpose of defeating or diminishing the effectiveness of an SEI process.

The work in [93] is one of the earliest–if not the first–work to investigate SEI threats. The authors examine threats that employ feature and signal replay to defeat modulation and transient-based SEI techniques. It is worth clarifying that the modulation feature replay is targeting constellation-based SEI, which leverages modulator imperfections such as IQ origin offset, wireless frame magnitude and synchronization (SYNC) correlation errors, or wireless frame phase error. Interestingly, the effectiveness of the threat's attack is nearly 100% when modifying and replaying modulation-based features. The authors also note that when a "high-end Arbitrary Waveform Generator" (AWG)–capable of sampling at 20 GHz–replays the signals of the targeted emitter, the transient-based SEI process struggles to distinguish the adversary from the emitter that is targeted by the adversary. However, these results are generated when the AWG and SEI process receiver is connected via wire, thus the authors note that the success of this attack will be diminished due to channel and antenna impacts. The authors do not present results validating this statement. They also conduct all of their experiments at a high SNR that is not specified but the distance between antennas is. It is also unclear as to whether or not the same receiver is used by the SEI process and the adversary but it seems that they are the same. Using the same receiver may provide the adversary with an unrealistic advantage because receivers impart signal coloration (see Section 7.2). However, further research is needed to determine whether this does in fact favor the adversary or not. Lastly, all of the emitters–adversary, SEI process, and targeted/legitimate–are the same model USRP SDRs. This also favors the adversary because it means that its RF front-end imperfections are most similar to those of the targeted emitter. Such a case is not realistic in IoT deployments because IoT devices are not likely to be implemented using SDR due to cost constraints. Thus, future research will need to consider cases in which the adversary uses an SDR but the targeted emitter is a Commercial-Off-The-Shelf (COTS) device.

The works in [49,109,129] investigate circumventing an SEI process through an adversary's ability to exploit a specific signal–and sometimes SEI–feature. The works in [49,109] look into an adversary's exploitation of CFO. CFO is defined as the difference between the frequency generated by the transmitter's LO and that generated by the receiver's LO. In communication systems, CFO is estimated and corrected for in the receiver prior to demodulation. CFO has been shown to be an SEI exploitable discriminating feature for emitters whose corresponding CFO distributions are unique amongst a set of known emitters [49]. An illustration of this is presented in Figure 3(a). The CFO distributions of Emitter #2 and Emitter #4 are unique (i.e., they do not overlap one another or those of the remaining emitters) while those of Emitter #1 and Emitter #3 do partially overlap. The latter case leads to Emitter #1 and Emitter #3 being confused for one another by the SEI process [49]. The results presented in [49,109] show that an adversary can easily monitor the CFO behavior of another emitter and then manipulate its own LO to obtain a similar CFO behavior–within its transmitted signals–that diminishes or even thwarts the SEI process' ability to distinguish the adversary emitter from the emitter targeted by the adversary.

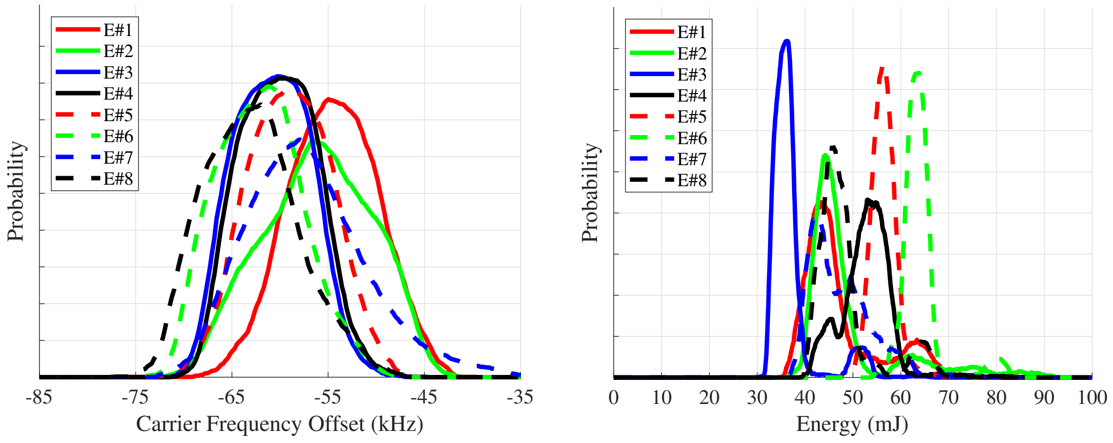

(**a**)CFO distributions. (**b**)Energy distributions.

Figure 3. Probability Mass Functions (PMF) for the receiver-incident Carrier Frequency Offset (CFO) and energy measured from eight Commercial-Off-The-Shelf (COTS) TP-Link Archer T3U USB Wi-Fi emitters, denoted using E#.

The authors in [135,136] investigate an adversary's ability to spoof the SEI features of another emitter with the intent of posing as that emitter to (i) emulate a primary user within a cognitive radio network, (ii) circumvent a signal authentication system, and (iii) gain unauthorized access into a protected network. The authors investigate replay and Generative Adversarial Network (GAN) based signal spoofing. Assessment includes SEI performance when the adversary transmits without actively spoofing the SEI features of another emitter but simply transmits random signals. The SEI features targeted for spoofing are power and phase shift; however, the authors do not specify whether these features manifest in the signal or constellation domain. Against DL-driven SEI, the results presented show that the adversary achieves a spoofing attack success rate of 7.89% when transmitting random signals (a.k.a., naïve spoofing), 36.2% for the replay-based spoofing attack, and 76.2% for the GAN-based spoofing attack [135]. In [136], the authors extend their work of [135] to include MIMO configurations of two and four antennas employed by the adversary or the receiver conducting SEI. The GAN-based spoofing attack is capable of achieving an attack success rate of 88.6% and 100% when two and four antennas are employed by the adversary, respectively. The authors note that the adversary's attack success rate increases with more transmitter antennas, but is decreased when the SEI process' receiver employs more antennas. Thus, the success of the spoofing attack seems to improve as the adversary employs more sophisticated methods (e.g., GAN and MIMO.) Despite the value of the work presented in [135,136], there are some key observations that must be considered for the threat it poses to SEI-based IoT security approaches. First, all of the research appears to be conducted using simulation, because the authors never provide any hardware specifics (e.g., manufacture and model of the emitters.) Thus, the efficacy of the presented approach in spoofing the SEI features of an actual emitter (i.e., hardware implementation) will need to be explored. Second, the authors use power as one of the exploited SEI features, which faces the same issues as those faced by SEI systems relying upon CFO or energy [49,109,129]. Third, it requires the adversary's receiver to be placed within close proximity of the SEI process receiver. Close proximity was necessary to ensure that the two receivers experience the same or very similar channel conditions. This appears to be an unrealistic requirement within operational IoT deployments. In [136], the authors do assess the GAN-based spoofing attack's success rate when its location differs from that of the SEI process' receiver. As the adversary's receiver moves farther from the location of the SEI process' receiver the less effective the GAN-based spoofing attack becomes; dropping from 100% to 56.2%. Fourth, the SEI spoofing results presented in [135,136] require the adversary to employ a transmitter and receiver that are not co-located, thus requiring additional coordination, management, and resources that may increase the adversary's chances of being detected. Lastly, the authors do not specify the total number of emitters that can be or are exploited by the adversary and omit spoofing performance against individual emitters. This is important when considering that an adversary is going to exploit the "weakest link" in any security system, thus the adversary is going to look for the emitter whose SEI features most resemble its own, organic SEI features or are spoofed with the greatest effectiveness.

The intention of the work presented in [100] is to collaboratively manipulate–using DL–the constellation-based SEI features (e.g., offset between emitter mean and ideal constellation point) of an emitter (a.k.a., Alice) to make it easier for the receiver (i.e., the device performing SEI) to identify Alice from a collection of emitters that are of the same manufacturer and model as Alice. The goal is to overcome SEI limitations within large populations of emitters. The authors assume the existence of a "feedback channel" between Alice and the receiver (a.k.a., Bob) during the SEI training phase. The authors also assess their DL-driven SEI feature manipulation approach's performance using an adversary emitter–designated as Trudy–that is capable of spoofing Alice's SEI features with increasing levels of sophistication. A conclusion that can be drawn from the work in [100] is that the most sophisticated version of Trudy is capable of adding confusion into the SEI decision that subsequently forces Alice to modify its SEI features at the expense of degrading communications performance (i.e., poorer bit-error-rate, BER) between Alice and Bob. These results highlight a drawback to constellation-based SEI, which is the fact that the constellation is two-dimensional. The two-dimensional nature limits the amount of variability–intentional and unintentional–that can exist between emitters while simultaneously maintaining communications performance. It is this constrained variability that may be exploited by an adversary or group of adversaries, especially as the modulation scheme changes (e.g., going from 8-Quadrature Amplitude Modulation (QAM) to 32-QAM), because it reduces the distance between constellation points.

In [137] the authors present a Deep Neural Network (DNN) architecture–designated as *FIRNet*–that is purpose-built to attack wireless DL networks by spoofing the signal features of another emitter. Wireless channel impacts, the adversary's own signal features, and a threat model is considered when assessing *FIRNet*'s efficacy. The use of a threat model is key to assessing security countermeasures with specific objectives as well as vulnerabilities in mind and is often missing in SEI publications. The authors also consider both targeted and non-targeted adversarial attacks. In a targeted attack, the adversary attempts to make emitter E_i's signals be identified as originating from emitter E_j. While the adversary attempts to make emitter E_i's signals identified as originating from any emitter other than E_i in a non-targeted attack. The authors' approach considers two adversarial scenarios. The first assumes the adversary has unrestricted access to the DNN performing SEI and is designated as a "white box" scenario. The second scenario is a "black box" scenario in which the adversary does not have unrestricted access to the SEI-performing network. However, the black box scenario does assume the adversary has access to the SEI network's final layer activations. Additionally, *FIRNet* is trained with the SEI process' trained DNN integrated into its own training processes. Lastly, *FIRNet* is evaluated using five, "nominally-identical" USRP N210 SDRs. The fact that all of the emitters are of the same manufacture and model provides the adversary with the best chance of spoofing the other emitters' SEI features. This is because emitters of the same manufacture and model are constructed using the same components, sub-systems, and systems, thus there will be a greater similarity between the adversary's SEI features and those observed or learned from the signals of the remaining emitters. The adversary's use of an SDR is reasonable when considering the level of control it needs to have over its own emitter to implement an attack. However, the use of SDRs as user equipment does not represent the typical, low-cost emitters present in IoT devices. So, *FIRNet* or similar adversarial approaches need to be assessed using actual IoT device emitters or ones that are more in line with those used in IoT deployments to fully evaluate the threat's effectiveness to SEI-based security approaches.

The authors of [138] leverage an adversarial machine learning process–designated as Radiometric signature Exploitation Countering using Adversarial machine learning-based Protocol switching (RECAP)–focused on countering SEI. RECAP attempts to confuse an SEI process by (i) having multiple emitters transmit the same message simultaneously so their signals are synchronized in time, and (ii) employing protocol switching at the link and physical layers. Link layer protocol switching is implemented by having each device switch amongst its emitter's supported protocols. Physical layer protocol switching is achieved through distributed beamforming in which the transmitting emitters' signals are combined together to form a new set of SEI features. Adversarial machine learning is used to select which link layer protocol is used to transmit the next message as well as which devices participate in distributed beamforming. RECAP is an elaborate SEI threat that requires a lot of coordination and adds complexity to any device employing it. However, RECAP represents a strong adversary that warrants further consideration and study within the SEI research community.

The authors of [139] introduce *RF-Veil* an algorithm that randomizes an emitter's phase errors with the goal of making SEI robust against impersonation attacks while obfuscating the emitter's SEI features from non-cooperative receivers (e.g., eavesdroppers). Although the authors present *RF-Veil* as an SEI-based security enhancement it is not difficult to imagine that nefarious actors may employ it with the goal of obfuscating their own SEI features to prevent, hinder, or circumvent legitimate SEI-based security processes. The use of *RF-Veil* by nefarious actors is not considered by the authors of [139], so future research should explore such an application. There are a few things to consider based upon the work in [139]. First, the authors' work is focused on Channel State Information (CSI)-based fingerprinting. Although CSI-based fingerprinting is outside the scope of this survey, the work in [139] does raise the question as to how *RF-Veil* or a similar approach impacts the effectiveness of signal- and constellation-based SEI. Second, the authors focus solely on obfuscating an emitter's identity by randomizing its phase information, thus focusing on a singular feature. Does a phase-focused approach create a vulnerability that opens it up for exploitation or attack as highlighted by other SEI works that considered a singular feature [49,109,129]? What about SEI processes that leverage multiple features? How is their effectiveness impacted? Lastly, the authors of [139] do not consider degrading SNR or other channel impairments (e.g., multipath, interference, etc.). Such channel conditions must be considered whether *RF-Veil* is used for good or ill.

The research presented in [140] uses adversarial learning to manipulate the signals' IQ samples in real-time using online learning. The adversary uses only binary feedback–from the SEI process–to determine if its IQ manipulations are effective or not in spoofing the signal-based identity of one of the N_e emitters. The weights and biases of the adversary's generative network are adapted based on the SEI process' response. The authors in [140] assess their approach using both simulations and a hardware testbed constructed using eight Analog Devices Active Learning Module (ADALM) Pluto SDRs. Although the results presented in [140] are able to "fool" the SEI process at a high rate (e.g., 90% or higher at signal-to-noise ratios of 15 dB and above), the authors conclude that the adversary does not actually learn the SEI features of the targeted emitter. Thus, the approach's effectiveness may have more to do with the classification itself. Classifiers perform a one-to-many comparison between the input sample (a.k.a., signal or its representation) and each class' model that represents an emitter within the known set. The input sample is assigned to the class whose model results in the "best" fit (e.g., smallest distance, largest probability, etc.). However, this class assignment is made even when the fit is poor. It is also important to note that all of the emitters are SDRs of the same manufacturer and model, which includes the adversary's SDR. Using SDRs of the same manufacturer and model represents a best-case scenario when it comes to SEI feature manipulation because there is less feature variability amongst emitters that only differ in the serial number. Therefore, it seems to provide the adversary with the greatest chance of fooling the SEI process, because its own SEI features should be inherently similar to those of the emitter being spoofed and require the least amount of manipulation. The authors do not: (i) test the spoofing effectiveness of the adversary's organic SEI features (i.e., the adversary is not manipulating its own SEI features) or (ii) assess SEI performance when the adversary's emitter is not of the same manufacture and model as the spoofed emitter. The adversary's use of an SDR is intuitive because an SDR grants the SEI manipulating algorithm direct access to its IQ channels/connections before the analog transceiver (a.k.a., the RF front-end). However, it is unlikely that IoT devices will employ SDRs due to Size, Weight, and Power-Cost (SWaP-C) constraints. So, future SEI work should consider the adversarial approach presented in [140] while considering some or all of the challenges that have been highlighted here.

As with CFO, the work in [129] shows similar results and vulnerability, but in terms of the energy distribution associated with an emitter's transmitted signals. In other words, when an emitter's signal energy distribution is unique the SEI process can easily discriminate that emitter from all other emitters within the known set. However, an adversary can easily manipulate the energy used to transmit its signals to mimic the energy distribution of another emitter. Figure 3(b) provides an illustration of this in which the adversary–designated as Eve–has a signal energy distribution that underlies that of another, known emitter (a.k.a., Alice), thus allowing Eve to be identified as Alice by the SEI process [129]. As a matter of fact, SEI processes tend to learn the easiest feature or set of features that allow discrimination of one emitter from another within a set of known emitters. The work in [49,109,129] all demonstrate SEI processes that primarily exploit a single feature (i.e., CFO or energy) to facilitate emitter discrimination, but at the cost of making them susceptible to adversaries that are capable of taking advantage of this singular vulnerability.

Similar to the work in [139], the authors of [141] present a CFO obfuscation technique to prevent adversaries from performing SEI of Bluetooth Low Energy (BLE) emitters. However, we discuss the work in [141] here because it can also be used by adversaries to mask their own CFO features or behaviors. The work in [141] differs from the work presented in [139] in that the transmitter intentionally obfuscates the CFO by adding a randomly selected value to it and applying it to the entire BLE transmission. Additionally, the authors of [141] increase CFO variation across signals by running the transmitter's Phase-Locked Loop (PLL) in a "temporarily unlocked" state that has the PLL's Voltage Controlled Oscillator (VCO) operating in an open loop configuration. The VCO's open loop configuration allows the frequency to drift which results in an unpredictable amount of CFO being added to the signal above what was intentionally added. The result of this CFO obfuscation approach necessitates persistent observation and measurement for twenty-eight hours or more–of the obfuscating emitter's signals–before the corresponding CFO distribution's statistics can be learned. The authors go further by providing a circuit design for a Wi-Fi and BLE emitter that incorporates their proposed CFO obfuscation approach. The work in [141] further validates that CFO is a poor SEI feature due to the ease at which adversaries can passively learn CFO–even if it takes a day or more–as well as manipulate their own. However, a key value of the work presented by the authors of [141] is a circuit designed to defeat or hinder SEI. Future research needs to consider a similar approach or approaches focused on other SEI-exploited features as expressed by Equation (1).

The authors of [142] take a different approach to SEI attacks that is built on the observation that DNNs are easily tricked by perturbed input data. Such perturbations have been shown to reduce DNN effectiveness or cause the DNN to fail altogether [143]. The authors present attack and defense scenarios. For the attack scenario, the adversary can select from one of four perturbations Fast Gradient Sign Method (FGSM) [144], Projected Gradient Descent (PGD) [145], and Carlini & Wagner (C&W) adversarial attacks [146] but results are presented using only the FGSM perturbation approach. The authors suggest that the perturbations can be added to the IQ samples of the adversary's signals before the Digital-to-Analog Converter (DAC); however, the authors do not add the perturbations before the adversary's DAC and instead add them to the received signals (i.e., after the signals have been transmitted, traversed the channel, and been received). Thus, it is unclear how easily the adversary can implement the perturbation, the effects the channel and the RF front-ends of the adversary and receiver would have on the perturbation, as well as whether or not such perturbations would negatively impact the demodulation process. The latter observation is important because it is safe to assume that an adversary's activities would not cease once it has been incorrectly granted access to the IoT system/infrastructure. Thus, if the perturbations cause sufficient signal distortion or bit errors to prevent demodulation, then the value of the attack is minimized or rendered useless. Nonetheless, the adversary's FGSM-based perturbation attack does significantly reduce the SEI processes' ability to separate the adversary from the authorized emitters and does so without the need to collect another emitter's signals or knowledge of the SEI exploited feature(s). However, the authors state that the adversary's perturbations leverage characteristics of the targeted DNN but do not provide specific details of what these characteristics are, what happens if the adversary does not have this knowledge, or how this knowledge is obtained. The authors counter the adversary's attack through their defense scenario, which leverages adversarial training to improve DNN-based SEI performance by 60% or more. It is important to note that the SEI process does know the adversary through collected unperturbed signals. The authors do not consider DNN performance–with and without adversarial training–when knowledge of the adversary's unperturbed signals is removed.

Traditionally, SEI research has assumed the exploited features are difficult to mimic [54,82–84,147] and the emitter being identified is passive or benign. However, the works reviewed in this section indicate that this is no longer the case and that ongoing SEI research must consider and contend with strong adversaries. A strong adversary is defined here as an adversary that actively attempts to hide its own SEI features or manipulate them to subvert or impede SEI-based security approaches. Thus, it is imperative to assess future SEI processes with strong adversaries in mind while removing weaknesses that provide adversaries with points of exploitation (e.g., CFO, signal energy, feedback in way of acknowledgments, etc.). In addition, SEI must be employed in conjunction with other security mechanisms to develop a "defense-in-depth" (a.k.a., layered) IoT security approach built on the tenets of prevention, detection, and response, which are essential to any security strategy.

5. Specific Emitter Identification at Scale

This section summarizes publications focused on assessing SEI's efficacy in providing robust and effective PHY-based security in the face of a large number of emitters and the identification of those emitters across collections.

5.1. Increasing Number of Emitters

IoT deployments can and do consist of tens to hundreds of individual devices, thus any SEI-based security approach must maintain its effectiveness while contending with large deployments. The majority of SEI investigations have focused on proof-of-concept demonstration, thus SEI's effectiveness within a large set of emitters (e.g., fifty or more) has received little attention until recently. This change has been driven in part by DL's demonstrated success within the fields of natural language and image processing, and facial recognition in the presence of large training data sets such as the MNIST data set of handwritten digits. under ever-increasing amounts of data. This has been exacerbated by recent pushes to leverage DL for the purpose of spectrum management [148] and emitter identification [149] by the Defense Advanced Research Projects Agency (DARPA), thus the remainder of this section focuses on summarizing SEI works that consider thirty or more emitters.

The authors of [58] utilize a tuned, FIR filter and CNN to identify five, ten, fifteen, and twenty USRP emitters. The FIR filter taps are optimized during training along with the CNN's weights. The number of filter taps is set to three, five, and ten. Accuracy is measured in two ways (i) Per Slice Accuracy (PSA) and (ii) Per Batch Accuracy (PBA). PSA is the average accuracy when a single signal is inferred by the network. A batch is a set of consecutive slices, giving the network a longer sequence of IQ samples to learn from. This helps the network by allowing for more temporal features to be visible. For all number of emitters in the set, the SEI performance increases roughly 20% when the optimized FIR is introduced. When the FIR filter is implemented, the ability of an adversary to mimic a trusted emitter is decreased from 10% to approximately 1% in a set of twenty USRP emitters. When the number of emitters is increased to one hundred, the PBA increases by 30% when using an FIR filter consisting of ten taps. When training and testing on a set of five hundred Automatic Dependent Surveillance-Broadcast (ADS-B) emitters, the highest performance improvement is 82% using PBA with a set of three batches, one hundred samples per slice, and ten tap FIR filter. Similarly, the highest performance improvement is 55% when using the same parameters as the ADS-B set.

The authors of [150] use the Differential Constellation Trace Figure (DCTF) and Differential Interval (DI) to identify fifty-four Zigbee emitters. The DCTF is used for its ability to highlight differences unique to each emitter in the set. The authors propose using the DCTF's amplitude and phase. The two representations are then feature-reduced using either the Gini importance or Relief-F algorithm. The reduced feature sets are used to train a random forest classifier and a *k*NN. When classifying emitters at an SNR of 10 dB and the DI set to 80, the random forest had a higher accuracy than the *k*NN classifier with both the Gini importance and Relief-F algorithm reduced DCTF features. When classifying at a range of DI values, the minimum value to maintain a classification accuracy above 95% at an SNR of 5% is 40. When comparing the classification accuracy of the different methods at 5 dB, the accuracy using the amplitude and phase representation with no feature reduction was 97%. This method had the same accuracy as when the phase-only representation is used without feature reduction and when the amplitude and phase representation are used with feature reduction. The performance decreases to 66% when only amplitude is used without feature reduction. Though the authors do not draw this conclusion, the results in [150] reiterate that the signals' phase representations tend to be more robust against noise than amplitude representations.

The authors of [151] investigate improving SEI performance by removing the intentional structure from the received signals transmitted by eight, sixteen, and thirty-two COTS emitters. Intentional Structure Removal (ISR) is performed in two ways: (i) subtracting an ideally generated, IEEE 802.11a Wi-Fi preamble from each of the received preambles in the time domain (a.k.a., the residual representation or error signal [69]) and (ii) dividing the Fourier coefficients of an ideal preamble from each of the received preambles in the frequency domain (a.k.a., the response representation). The authors train an LSTM using a data set comprised of signals at SNR values of 9 dB and 30 dB. These SNR values are achieved by adding realizations of scaled, white Gaussian noise to the received preambles. The authors assess SEI performance using signals that have or have not undergone time or frequency domain-based ISR. The highest SEI performance–when identifying eight emitters–is achieved using the received signals' response representation. When the number of emitters increases to sixteen, SEI performance decreases from 58% to 42% in the frequency domain without ISR at an SNR of 9 dB. When the response representation is implemented, SEI performance decreases from 62% to 48%. When identifying thirty-two emitters, SEI performance is 40% without ISR and 46% when using the response representation at an SNR of 9 dB. Interestingly, when using the residual representation, SEI performance is higher with thirty-two emitters than when identifying sixteen emitters using the received signals (i.e., ISR is not performed). The authors show that removing the received signals' intentional structure allows the DL network to learn each emitter's RFF features without confusion imposed by the intentional signal structure, thus improving SEI performance as the number of emitters increases.

Based on the papers reviewed in this section as well as the work presented in [152], it is clear that SEI-based security solutions face a scalability problem in that as the number of emitters increases the SEI performance suffers. This observation is reinforced by the authors of [153] who state that DL-based model accuracy decreases as the number of to-be-identified emitters increases. The question is whether or not this is a problem with DL or one that plagues even traditional machine-learning approaches. Literature has stated that DL performance improves as the amount of data increases [154] but for DL as it is applied to natural language processing, facial recognition, spectrum management, and not SEI. So, future research is needed to address this challenge and the solution may not rest with the DL or machine-learning algorithm(s) but with the signals, their representation, or the *uniqueness* and *permanence* of the SEI-exploited features.

5.2. Cross-Collection SEI

Cross-collection SEI refers to the case in which emitter-specific features are learned from a single set of collected signals by a machine learning algorithm and then used to identify the same set of emitters using signals collected at another time. Typically, cross-collection SEI involves signals collected over multiple sessions which can span hours, days, weeks, or more. It is important to note that cross-collection SEI assumes the same receiver is used for all signal collections. Cross-receiver SEI is designated herein as receiver-agnostic SEI and is addressed in Section 7.2.

The work in [152] analyzes the effect of IQ channel balancing on cross-collection classification performance across ten thousand emitters. This work utilizes Per-Transmission Accuracy (PTA), and PSA. When using PTA, the entire Wi-Fi QPSK signal's IQ samples are input into the network. When PSA is used, each signal is sectioned off into portions, and each portion is input into the network. The emitter with the most classifications across all portions is chosen as the classification for that given signal. In the first experiment, a CNN with ten stacked convolutional layers is trained to identify devices from a set of thirteen USRP N210s and seven X310s. When trained on a single day out of ten days, the average day-zero PSA is 99%. When identifying the same emitters by their signals collected on the remaining nine days, the average PSA falls to 5% with a maximum accuracy of 6% without IQ channel equalization. When IQ channel equalization is performed, the average day-zero PSA falls to 99.5% while the average PSA when classifying the remaining days increases slightly to around 6% with a maximum of 12%. When the number of Wi-Fi devices increases to three hundred and fifty, the ResNet-50-ID CNN is able to classify Day Zero data with an average PTA of 74.5% and a PSA of 44.1%. When classifying signal collection on another day, the PTA and PSA fall to 1.2% and 1.3%, respectively. When utilizing IQ-channel equalization, the PTA and PSA when classifying on a new day increases to 17.5% and 25.8%, respectively. The ten-layer CNN has a PTA of 23.2% and PSA of 22.5% when classifying signal collected on days other than Day Zero and IQ channel equalization is employed. The authors conclude that the drop in classification performance–when training using one day's worth of collected signals and testing using another day's collected signals–is due to the non-stationary nature of the wireless channels that the Wi-Fi emitters communicate over.

The authors of [155] investigate the effect of traditional wireless channel mitigation techniques on cross-collection SEI. Ten thousand IEEE 802.11a Wi-Fi preambles are collected from thirty-two TP-Link Archer T3U USB Wi-Fi dongles over eight days with one week between collections (i.e., signals are collected every Friday). The first experiment trains a CNN on a combination of real, imaginary, magnitude, and phase components of the preambles' time and frequency domain representations. A total of n-choose-k components are used where $n = 8$ (i.e., four from each representation), and k is incremented from one to eight in steps of one. A total of two-hundred and fifty-five representations are trained and tested. When ranked by the highest cross-collection accuracy, the feature combinations containing the frequency components ranked higher than combinations comprised primarily of time domain components. The combination of all four frequency components is ranked nineteenth with an accuracy of 18.56%, and the combination of all time components is ranked one-hundred and ninety-eighth with an accuracy of 16.41%. Based on these results, the authors chose to use only the four frequency components for the remainder of the experiments because they represent only 33% of the total data while reducing the cross-collection SEI performance by approximately 0.7%. When using the frequency representation's real, imaginary, magnitude, and phase components, average SEI performance across all collections fell by 0.75% to 18.56%. While the four, time domain components result in an average accuracy is 16.41%. The authors also perform SEI using CNNs with depths of one, two, four, eight, sixteen, and thirty-two stacked convolutional layers using all four frequency components and only Day Zero collected signals. The single convolutional layer CNN achieves an average SEI performance of 15% across all collections and the four convolutional layer CNN achieves the highest average accuracy of 18.57%. Next, n-choose-k preambles collected on Day Zero are selected for training where $n = 10,000$ preambles and the values of k are set to 1,000, 2,000, 5,000, and 10,000. From these selected preambles, one, two, four, eight, and sixteen 30 dB AWGN realizations are generated to simulate multiple instances of the wireless channel for network training. When training on one realization of 1,000 preambles, the average SEI performance when classifying each emitter's Day Zero collected, 10,000 preambles is 55%. When training on sixteen noise realizations added to the same set of 1,000 preambles, average SEI performance increased to 61.43%. When the number of preambles is increased to 2,000, average SEI performance increases to 64.77% with only a single noise realization. When training on a single realization and 10,000 preambles, average SEI performance increases to 95%, showing that real-world collected signals allow the network to generalize better than multiple, simulated noise realizations. When training on 10,000 preambles per emitter collected on Day Zero and classifying across all collections, the accuracy is 19.78% with one noise realization and 22.59% when using sixteen noise realizations. Training on sixteen noise realizations also increases the training time by a factor of sixteen, showing that there are diminishing SEI performance gains for a large increase in training time. Channel effect motivation is investigated through the use of STS symbol averaging. When using STS symbol averaging, cross-collection SEI performance is 20.8% when only the averaged symbol is re-inserted into the preamble, 20.48% when the average STS symbol is replicated and re-inserted into the preamble, and 20.32% when only the replicated STS symbol is used all of which are below the average SEI performance of 21.53% without STS averaging. Next, the authors use a residual representation of the preambles. In this study, the residual is calculated by dividing the first through fifth STS by the sixth through tenth STS, then dividing the first LTS by the second LTS, and finally concatenating the two resulting portions. The residual preamble results in a drop in average SEI performance from 20.71% to 11.62%. Finally, the number of collection days represented in the training set is increased from one to seven–in increments of one day's worth of signals–to provide the CNN with a greater presentation of the possible SEI feature variation that can occur across an emitters' transmissions over multiple collections. When training on Day Zero collected signals the average SEI performance when classifying all collections is 20.32%. When adding the second day's signals to the training set, the average SEI performance increases to 38%. This trend continues as each subsequent day's collected signals are added to the training set which ultimately results in an average SEI performance of 94.4% when the first seven collections are used for classifying all eight collections. Despite this, Day #8's average SEI performance is never more than 30% when five or more days' worth of preambles are included in the training set. This is 22% higher than the same collection's classification accuracy of 9% when only Day Zero's collections are used to train the network. The authors conclude that current DL-based SEI techniques cannot adequately learn a general representation of an emitter's RFF features to achieve high accuracy performance across multiple signals collections.

The authors of [156] leverage Adversarial Domain Adaption (ADA) and device rank to improve emitter classification performance between a set of (i) twenty USRP and (ii) ten HackRF One SDRs. The ADA algorithm utilizes transfer learning between a source, Day #1, and a target, Day #2, data set. Training is conducted on an (i) Feature Extractor F, (ii) Domain Discriminator D, and (iii) Source Classifier C. F highlights the coloration within a specific emitter's signals passes them to D and C. D classifies the signals in terms of whether it is the source or target while C aims to correctly identify the originating emitter. The goal of F is to maximize the accuracy of C and confuse D with the goal of highlighting domain-invariant features. The parameters of F, D, and C are updated using back-propagation until a target performance level is met. F is then attached to a kNN classifier. F's parameters are frozen and the kNN's parameters are updated to minimize error when classifying the target data set (a.k.a., Day #2). Device rank is a method of identifying an emitter using multiple portions of its collected signal. When classifying, each portion is independently assigned a class by the classifier. The emitter that has the most assignments is the overall classification decision. This is the same approach as the PSA method utilized in [152]. The authors also investigate the effect of the window and stride length when using the device rank approach and a CNN. The highest Day #1 accuracy is achieved with a window length of 288 and a stride of 1. As the stride length across the IQ signal increases, the Day #1 accuracy decreases significantly. Day #2 performance for the USRP data set did not change with the stride length. SEI performance increases from 20.4% to 26.23% when the stride length increased from 1 to 576 samples when using the HackRF One data set. When the CNN is replaced with ADA, average SEI performance increases from 8.41% to 43.17% when using the USRP data set, and from 25.98 to 65.24% when using the HackRF One data set. The authors attribute this performance increase to the robust nature of the ADA algorithm but the presented results presented are not the result of blind testing. The CNN-only method is trained using Day #1 signal collections while the ADA is trained using signals collected on Day #1 and Day #2, thus resulting in an unfair comparison because the ADA's SEI results correspond to validation testing while the CNN's SEI results correspond to blind testing.

The authors of [157] use Zero-Shot Learning (ZSL) to cluster unknown, unlabelled emitters. ZSL first learns SEI features of a known, trusted emitter set and maps the emitters into clusters. When new data is presented to the classifier, it either falls into a known cluster and is identified as the emitter assigned to that cluster, or does not fall within a known cluster and is held out as a new emitter. ZSL allows for new clusters to be generated online. The authors use eight USRP B210 SDRs. The receiver, sampling frequency, and whether CFO is removed are unclear. Training is performed with a CNN, Multi-Layer Perceptron (MLP), and an AutoEncoder (AE). Five emitters are selected and designated as known while the remaining three are held out as unknown. Once trained, each NN's activation is passed to the clustering algorithm. Once trained using the known emitters' signals, the clustering algorithm is trained using the unlabelled, unknown emitters' signals. SEI performance is determined based upon the clustering algorithm's ability to sort and accurately assign each of the unknown emitters to their own, unique cluster. Neither the NNs nor the clustering algorithm achieves a blind test accuracy above 50%. Average SEI performance is around 33%, which is a guess when classifying the three unknown emitters. The authors conclude that SEI networks are not able to uniquely identify previously unseen emitters well.

Based on the reviewed work, it can be concluded that a solution for cross-collection SEI has not been found. It can be concluded that a large factor contributing to the poor performance–when classifying a new set of collected signals–is due to the non-stationary nature of the wireless channel. This channel is not sufficiently modeled by AWGN noise realizations, but the networks generalize better when training on more real-world, collected preambles. Until cross-collection SEI performance improves, the current methods, whether based on traditional or deep learning, are not sufficient for securing IoT deployment over multiple collections thus throwing the *permanence* of SEI exploited features into question.

6. SEI Data Sets

This section provides a summary of signal data sets that have been used to generate SEI results in published papers and that the authors have made available to the SEI research community to aid further advancements within the topic area as well as to serve as benchmarking data sets.

1. **POWDER Signals Set:** The Platform for Open Wireless Data-driven Experimental Research (POWDER) signals set is used to evaluate SEI performance in vendor-neutral hardware deployments of 5G and Open Radio Access Networks (ORANs) [158]. The new paradigm in 5G and ORANs includes emitters transmitting different protocol signals such as 5G, Long-Term Evolution (LTE), and Wi-Fi at different times. The work in [158] evaluates SEI as a PHY layer authentication technique in such networks using over-the-air signals collected by the large-scale POWDER platform. The signals set includes IQ signal samples collected from four base stations located in different geographical areas. Each base station is implemented using an Ettus USRP X310 SDR and is used to transmit standard-compliant IEEE 802.11a Wi-Fi, LTE, and Fifth Generation-New Radio (5G-NR) frames generated using MATLAB®'s Wireless Local Area Network (WLAN), LTE, and 5G toolboxes. A USRP B210 SDR–located at a fixed point–collects the signals transmitted by the four base stations at a sampling frequency of 5 MHz for Wi-Fi and 7.69 MHz for LTE and 5G. For each base station, the receiver is used to collect IQ samples for two independent days. A single-day collection is comprised of five sets of IQ samples per base station and protocol, each two seconds in duration. The data is stored in binary files using Signal Metadata Format (SigMF). Each SigMF file consists of a metadata file containing a description of the collected signals and a data file holding the actual collected signals' IQ samples.
2. **DeepSig RadioML Signals Sets:** These signals sets are used to evaluate the classification performance of emitter signals in [63,159]. The work in [63] studies the effects of symbol rate and channel impairments on RF signals classification performance by (i) simulating the effects of CFO, symbol rate, and multipath as well as (ii) measuring over-the-air classification performance using software emitters. The signals set used in [63] captures twenty-four different digital and analog single-carrier modulation schemes including On-Off Keying (OOK), 4-ary Amplitude Shift Keying (ASK), 8-ary ASK, Binary Phase Shift Keying (BPSK), Quadrature Phase-Shift Keying (QPSK), 8-ary Phase Shift-Keying (PSK), 16-ary PSK, 32-ary PSK, 16-ary Amplitude and Phase-Shift keying (APSK), 32-ary APSK, 64-ary APSK, 128-ary APSK, 16QAM, 32QAM, 64QAM, 128QAM, 256QAM, Amplitude Modulation-Single Side-Band-Without Carrier (AM-SSB-WC), AM-SSB with Suppressed Carrier (AM-SSB-SC), AM-Double Side-Band (DSB)-WC, AM-DSB-SC, Frequency Modulation (FM), Gaussian Minimum-Shift Keying (GMSK), and Offset Quadrature Phase-Shift Keying (OQPSK). The resulting modulated symbols are shaped using a root-raised cosine pulse shaping filter. To simulate a time-varying wireless channel, channel parameters such as Rayleigh fading delay spread are randomly initialized before each transmission. The signals are transmitted and collected using USRP B210 SDRs in an indoor channel on the 900 MHz Industrial, Scientific, and Medical (ISM) band for the over-the-air portion of the signals set. Each captured signal in this data set is comprised of 1,024 samples. The signals of two-million samples are encoded using the hdf5 file format.

Another DeepSig signal set was generated by the authors of [159]. The authors of [159] investigate the feasibility of applying machine learning to the signal processing domain. The authors use the GNU Radio platform to generate a synthetic collection of signals with varying SNR and eleven types of analog and digital modulation including 8-ary PSK, AM-DSB, AM-SSB, BPSK, Continuous-Phase Frequency-Shift Keying (CPFSK), Gaussian Frequency Shift Keying (GFSK), PAM4, 16QAM, 64QAM, QPSK, and Wide-Band FM (WBFM). For the analog and digital portion of the signal set, the authors use a continuous data source from acoustic voice speech and Gutenberg's works of Shakespeare in ASCII, respectively. The data is organized in a multidimensional float32 vector with a size of,

$$N_s \times N_c \times D_1 \times D_2, \tag{2}$$

where N_s refers to the number of signals. N_c is set to one, $D_1 = 2$ referring to the I and Q channels, and $D_2 = 128$ is the number of samples in each signal. The four-dimensional data set is stored in cPickle format to facilitate access and integration of machine learning platforms such as Keras, Theano, and TensorFlow.

3. **ORACLE Signal Set:** This set of signals was collected by the authors of [160] to evaluate their Optimized Radio clAssification through Convolutional neuraL nEtworks (ORACLE) approach. The authors of [160] evaluate the classification (identification) performance of the proposed approach within static and dynamic channels that are simulated using MATLAB® toolboxes. The ORACLE data set includes signals collected from sixteen USRP X310 emitters that are transmitting IEEE 802.11a Wi-Fi-compliant frames. A stationary USRP B210 SDR is used to collect all of the IEEE 802.11a Wi-Fi frames at a sampling frequency of 5 MHz and a center frequency of 2.45 GHz. More than twenty million signals are collected for each emitter. Each signal is divided into length 128 sub-sequences and stored as float64 in binary files.
4. **WiSig Signal Set:** This signal set is generated by the authors of [161] and includes ten million IEEE 802.11 Wi-Fi signals collected from 174 COTS Wi-Fi emitters using forty-one USRP receivers over four captures representing four different days. The authors of [161] attempt to address degrading SEI performance due to channel variations caused by the use of different receivers or signals collected over multiple days. The Wi-Fi signals sent by 174 Wi-Fi nodes to the Access Point (AP) are captured by forty-one USRP receivers including B210s, X310s, and N210s. To create the raw WiSig data set, four single-day captures were performed and combined to generate a 1.4 terabyte data set. The collected, raw signals are prepossessed to extract the first 256 IQ samples from each Wi-Fi frame with and without channel equalization. The steps and scripts to preprocess the collected signals are provided by the authors along with the data set. For convenience, the authors of [161] subdivided the data set into four smaller subsets:

   - **ManyTx:** contains fifty signals for each of the 150 emitters and the signals collected by eighteen receivers over a four-day period.
   - **ManyRx:** contains 200 signals for each of the ten emitters and the signals collected using thirty-two receivers over a four-day period.
   - **ManySig:** contains 1,000 signals for each of the six emitters and the signals collected using twelve receivers over a four-day period.
   - **SingleDay:** contained 800 signals for each of the twenty-eight emitters and the signals collected by ten receivers in a single day.

   The WiSig signal set signals are detected using auto-correlation performed using the Wi-Fi preamble's STS portion and re-sampled to a rate of 20 MHz.

One of the biggest challenges with any machine learning-based research is access to data. The data sets summarized above are some of the largest and the few that are publicly available for use in SEI research activities. One of the drawbacks to these data sets is that the signals are transmitted by SDR-based emitters, which do not reflect typical emitters employed by IoT devices. So, there remains a need for public data sets of signals collected from COTS emitters used by IoT devices or in IoT deployments.

7. Considerations for SEI in IoT Deployments

IoT devices are typically constrained in terms of power, memory, computation, or combinations thereof to keep the cost of the IoT device down, increase the operating lifetime by extending or maximizing battery life, or both. In this section, we summarize SEI works that consider these constraints.

7.1. SEI On Resource Constrained Devices

The authors of [162] present one of the earliest SEI approaches designed to reduce or alleviate computation, energy, and communications overheads associated with performing SEI-based security approaches on resource-constrained IoT devices. The authors accomplish this by offloading the SEI task to cloud and edge devices or resources. Initial CNN training is performed in the cloud and once trained the CNN is mutually re-trained and made sparse through the use of a progressive weight pruning algorithm [163], thus the authors focus on reducing computation and energy requirements during the testing or inference stage instead of during CNN training. The re-trained and pruned CNN is then deployed to the edge to run on a gateway or another IoT device that is responsible for relaying information. The authors assess the pruned model's computation and energy reduction performance using a Samsung Galaxy S10, an NVIDIA Jetson TX2 Module, and a Xilinx-ZCU104 Field Programmable Gate Array (FPGA). The authors use two data sets comprised of 500 IEEE 802.11 b/g/n Wi-Fi emitters with 273 signals per emitter and fifty ADS-B emitters with 273 signals per emitter. The authors perform SEI using a derivative of the ResNet architecture [164] and assess it and its pruned versions in terms of average percent correct performance, pruning rate, and the number of Floating Point Operations Per Second (FLOPS). Using a pruning rate of 5.4× results in a 0.96% drop in average percent correct classification performance–61.4% for the full ResNet versus 60.44% using the pruned ResNet–while reducing the number of FLOPS by 20% when identifying the 500 Wi-Fi emitters. For the ADS-B data set, a pruning rate of 5.4× results in a 0.25% drop in average percent correct classification performance–88.53% for the full ResNet versus 88.25% using the pruned ResNet–while reducing the number of FLOPS by 19.3%. Regarding the three hardware platforms, the presented approach increases classification speeds by as much as three times on the Samsung Galaxy S10 and eleven and a half times on the FPGA. The authors only present average classification performance results. Hence, it is difficult to determine how evenly distributed the performance is across individual emitters and do not assess their approach under degrading SNR conditions, but do pose techniques to address the latter under future efforts. However, the biggest concern surrounding the approach in [162] is their use of CFO. CFO is estimated and removed before channel equalization but reinserted once equalization is concluded. CFO's presence is a vulnerability that SEI adversaries can exploit, see Section 4 for details. So, it would be interesting to see how the results presented in [162] would change if CFO is not reinserted. Despite this, the work in [162] does provide a viable means of reducing SEI's burden on edge, IoT devices and shows that SEI can be successfully employed on smartphones.

In [165], the authors present an IoT resource allocation approach that leverages SEI-based security. In particular, the authors focus on IoBT deployments but as previously stated IoBT is a form of IoT, thus we only use IoT in our article. The authors' approach aims to improve IoT network Quality of Service (QoS) through the use of SEI and by optimizing network performance. The former is of particular interest here and the authors propose SEI as a means of controlling user access in .lieu of traditional cryptographic approaches because cryptography systems have higher computational requirements, which limit their use in IoT deployments. Specifically, SEI is used to improve IoT network QoS by identifying and removing malicious users/devices that launch Distributed Denial-of-Service (DDoS) attacks aimed at reducing available network resources (a.k.a., power and channel allocations). Such resources are often limited in IoT deployments and their reduction negatively impacts network performance optimization. The authors optimize network performance by calculating the IoT network's utility. The utility is calculated using many parameters including but not limited to the number of sensing devices, power consumption of RF circuits, transmit power of the considered devices, data rate(s), and per-device channel allocation. However, the authors do not seem to consider how performing SEI impacts IoT network utility. It may be that performing SEI is "lumped" into another parameter such as RF circuit power consumption. If it is, then it is unclear whether SEI is to be performed on individual IoT devices or the proposed centralized server. Either way, a specific parameter or parameters associated with the performance of SEI should be integrated into the IoT utility optimization calculation and contrasted against the use of cryptography–instead of SEI–to highlight the benefit of SEI-based security in IoT deployments. Lastly, the authors do not present any SEI-related results, which–from a purely SEI viewpoint–seems to limit the contributions of the approach. However, this can be easily remedied by integrating SEI into the IoT network utility optimization calculation.

The authors of [166] make note of the fact that recent advancements in SEI have been made through the use of DL at the cost of large numbers of hyperparameters that are updated via time-consuming backpropagation along with the fact that DL structures are not scalable making them computationally expensive, thus limiting the practicality of DL-based SEI in IoT devices and infrastructure. The authors attempt to address these DL-related issues by proposing an SEI approach built on a Broad Learning System (BLS) called Adaptive Broad Learning (ABL). ABL trades the depth of a DNN for width by increasing the number of nodes that comprise the node layer, replaces time-consuming backpropagation with the pseudo-inverse calculated from the node layer to the output layer, and updates only the new nodes instead of all of the nodes when the network needs to be modified. ABL consists of a node layer–that is comprised of feature and enhancement nodes–and an output layer. The feature nodes work directly on the signal's raw IQ samples while the enhancement nodes' inputs are the output of the feature nodes. The authors assess ABL's SEI effectiveness using two publicly available data sets from [167,168]. The authors' results show that ABL's average SEI performance is on par with the best DL approaches using the first data set [167] and slightly above average when using the second data set [168]. Regarding the second data set performance, the authors attribute the poorer performance to the higher sampling rate, which creates feature redundancy that provides an edge to the DNN architectures. The real benefit of ABL is the reduction in training time, which is a fraction of the time needed to train the DNNs. The authors' approach is novel but a few considerations must be made. First, the authors note that ABL requires massive, labeled data sets for training, thus limiting its usefulness in which previously unseen emitters are present in the operating environment. In today's environment of increasing and ubiquitous IoT device deployments, the presence of previously unseen emitters seems inevitable. Second, the authors state that the presence of redundant information within the signals causes ABL to overfit. Lastly, one must keep in mind that training does not have to be performed on the IoT device but instead can be performed at a central location initially, and to perform updates, thus the SEI-performing device would only need the latest, trained model. Despite this, ABL is an interesting approach and further research is warranted due to its novelty within the SEI space.

Similar to the work in [166], the authors of [169] approach SEI using a broad learning network to lower computational load on the end device to address resource constraints associated with IoT integration. However, the work in [169] differs through the use of signal feature embedding instead of the node expansion approach in [166]. The authors [169] call their broad learning-based SEI approach Signal Feature Embedded Broad Learning Network (SFEBLN). Signal feature embedding intends to approximate the SEI features through the use of a nonlinear transformation with the intent of improving SEI performance. Signal features are generated by performing signal processing before and within the broad learning network. Signal convolution, windowed pooling, and signal shifting are performed before the broad learning network while internal signal processing consists of calculating the Discrete Fourier Transform (DFT), Discrete Cosine Transform (DCT), and the Short-Time Fourier Transform (STFT). Additionally, the authors perform broad learning-based SEI using a Central Processing Unit

(CPU) to show the feasibility of performing SEI without the need for a Graphical Processing Unit (GPU). Assessment of SFEBLN is conducted using a set of ADS-B signals and compared with SEI performed using three DL-based approaches, the ABL approach from [166], and two traditional, handcrafted SEI approaches. The DL-based SEI approaches are a real-valued CNN, complex-valued CNN, and the multi-scale CNN from [170]. Traditional, handcrafted SEI is performed using random forest and Support Vector Machines (SVM). The authors consider six scenarios in which the SEI processes each identify 10, 20, 30, 50, 100, or 200 individual ADS-B emitters. SFEBLN results in superior average percent correct classification over both handcrafted, real-valued CNN, and multi-scale CNN approaches for all six identification scenarios. SFEBLN is also superior to the complex-valued CNN–in terms of average percent correct classification performance–when identifying 40 or fewer ADS-B emitters. The true benefit to SFEBLN is its time advantage over the six alternate SEI approaches. SFEBLN can be trained in less than 10 seconds when 100 or fewer ADS-B emitters are represented in the training set and in less than 13 seconds when 200 emitters are represented. For SNRs of -10, -5, 0, 5, and 10 dB, the average percent correct classification performance of SFEBLN is superior to all alternate SEI approaches except for the case of 200 ADS-B emitters at an SNR of -10 dB. For this exceptional case, the complex-valued CNN proves to be roughly 10% better but at the expense of huge computing overhead (roughly 2,000 times). The authors do identify a drawback to SFEBLN, that it is susceptible to instability in its results due to the random initialization of the single-layer weight, and that this instability is exacerbated by such things as temperature, multi-threading, and other unspecified factors. To address this, the authors assess SFEBLN stability using Monte Carlo simulation while considering impacts on accuracy, training, and testing times. The authors show that SFEBLN stability remains within acceptable limits but they do not perform the stability assessment under degrading/low SNR conditions, thus it is difficult to determine if SFEBLN will remain stable as SNR decreases. Also, the authors of [169] do not address any of the concerns raised by the authors of [166] and highlighted in the previous paragraph.

The authors of [171] design their SEI approach using a systems view to make it better suited for real-world operations. The authors consider training data availability, robustness to unknown operational conditions and uncertainty, channel conditions, and computation limitations. The authors address limitations associated with training data availability by acknowledging that data distributions will change between the training and testing phases, using simulated data for training and fine-tuning using real-world data, integrating detection of unknown emitters, and using a limited number of training examples per emitter. The robustness to unknown operational conditions and uncertainty limitations are addressed during training by using a large data set and then tuning or adapting the deployed version, a data set comprised of multiple, distinct signal types (e.g., Wi-Fi and ZigBee), and a data set containing signals that represent spoofers, or other signals in the area of deployment. Channel condition limitations are addressed by including corrupted signals in the training data. In particular, the authors include signals that are overlapped in time and spectrum with other signals of the same type and SNR with only the amount of overlap changing, and other information to improve performance by leveraging other receiver capabilities such as the direction of arrival. The authors address the final limitation–computation–by lowering the bit precision of the network weights, the network's depth, the number of filters per layer, and network pruning. The work in [171] is not without its limitations. Primarily, the data they used is not publicly available [149] and the DL network used is developed by a private company, BAE Systems Inc., which could limit the SEI research community's access to it.

The authors of [172] present a data reduction approach that leverages entropy to select the most informative portions of a signal's Time-Frequency (TF) representation. The signal's TF representation is a normalized, grayscale image generated from its GT's complex-valued coefficients. A GT image's most informative portions are selected by comparing a portion's (a.k.a., patch) entropy value to the entropy value of the entire image. If a patch's entropy is equal to or greater than the image's entropy value, then that patch is retained for subsequent SEI. If it is lower than that of the image's entropy value, then the patch is discarded. The presented entropy-informed SEI approach outperforms SEI processes that use the signal's raw IQ samples and are comparable to those that use the full, GT image at SNRs of 15 dB or greater. When compared to the whole, GT image-based SEI approach, memory usage and CNN training times are reduced by 93% and 81%, respectively.

The authors of [173] look to lower the SEI burden on IoT devices and the supporting network by investigating DL-based upsampling impacts on SEI performance. In particular, the authors investigate using a Conditional Generative Adversarial Network (CGAN) to upsample the signals collected by IoT devices that measured them using a lower sampling rate. Allowing the IoT device to collect the signals at a lower sampling rate aligns with current IoT design practices [174]. The authors use the CGAN to upsample IEEE 802.11a Wi-Fi preambles collected at sampling frequencies of 2.5 MHz, 5 MHz, or 10 MHz to a sampling frequency of 20 MHz and compare results generated from the upsampled signals to those generated using signals sampled at 20 MHz during collection. They compare SEI results generated using signals upsampled using two other conventional interpolation methods known as piece-wise Linear Approximation Interpolation (LAI) and Cubic-Spline Interpolation (CuSI). Additionally, the CGAN upsampled signals' SEI results are compared to those generated using a CNN and the organic sampled signals (i.e., the signals are not upsampled before conducting SEI). The greatest improvement in average percent correct classification performance is achieved when the signals collected at a sampling rate of 5 MHz are upsampled to 20 MHz. The 5 MHz sampled signals result in an average percent correct classification performance between 84% and 95% for SNR values ranging from 9 dB to 30 dB, respectively. While the CGAN upsampled version of the 5 MHz signals results in an average percent correct classification performance between 92% and 98% over the same range of SNR values. However, the use of signals collected at a sampling frequency of 20 MHz results in better performance over those upsampled by the CGAN from 5 MHz to 20 MHz, especially at SNR values below 21 dB. Despite this, the work in [173] provides a potential approach for lowering the resource demands (e.g., memory, power, computation) placed on individual IoT devices; however, SEI performance improvements are needed and the number of devices increased.

In [175], the authors present an active Distinct Native Attribute (DNA) fingerprinting process capable of identifying legitimate and counterfeit Wireless Highway Addressable Remote Transducer (HART) adapters using sub-Nyquist sampled signals. The work in [175] differs from that in [173] in that the signals are never upsampled or interpolated. It also differs from the other papers cited in this survey in that the emitters under test are stimulated and DNA fingerprints are generated or learned from the resulting response(s). In other words, the collected responses are not necessarily produced during normal, unstimulated operations, and are collected using a wired setup although assessment is conducted under simulated, degrading SNR conditions. It is also worth noting that the active DNA fingerprinting process in [175] serves a different purpose than passive SEI processes–including those cited in this survey–in that the work in [175] focuses on identifying counterfeit Wireless HART emitters within the pre-deployment portion of their life cycle to ensure or maintain supply chain integrity. In contrast, passive SEI approaches are primarily focused on securing communications networks during the deployed/operating period of the emitters' life cycles. The authors of [175] perform DNA fingerprinting using a traditional Multiple Discriminant Analysis (MDA) and CNN-based classifier. For MDA-based DNA fingerprinting, the sub-Nyquist signals' time domain representations of magnitude, phase, and frequency are calculated, each is subdivided into eighteen equal-length sub-regions, the statistics of variance, skewness, and kurtosis calculated for each sub-region, statistics of each sub-region are sequentially concatenated together along with the statistics calculated across the entirety of each time domain representation, and all statistics from each time domain representation concatenated together to form a DNA fingerprint. For CNN-based DNA fingerprinting, the same time domain representations are calculated for each sub-Nyquist signal but no further processing is conducted, which leaves feature learning and selection to the CNN. The authors of [175] consider both one- and two-dimensional CNN-based DNA fingerprinting. The one-dimensional case uses only the time domain DNA fingerprints. While the two-dimensional CNN-based DNA fingerprinting uses both the time and frequency domain representations of the sub-Nyquist signals. The authors do include results generated from Nyquist-sampled signals to facilitate comparative assessment. In the end, the two-dimensional CNN-based DNA fingerprinting process proves superior in identifying legitimate Wireless HART emitters at an average percent correct classification rate of 91.6% or better at SNRs of -9 dB and higher. This same process correctly identifies counterfeit emitters at an average rate of 91.5% or higher at SNRs of -9 dB and higher. These results are achieved at a sub-Nyquist sampling rate of 1/205th that of the Nyquist rate. The Wireless HART signals are collected at a sampling rate of 1 GHz, which yields a sub-Nyquist rate of roughly 4.88 MHz. When considering the sub-Nyquist sampling rate and the results presented by the authors of [175], the presented sub-Nyquist DNA fingerprinting process appears to provide a viable method for alleviating or reducing the burden that the current Nyquist and higher sampling rate-based passive SEI approaches place on IoT devices and infrastructure.

The authors of [176] present a lightweight SEI approach built on the Gated and sliding Local self-attention transFormer (GLFormer). The authors' approach is inspired by the successful use of the Transformer [177] a self-attention mechanism that provides DL architectures the ability to capture interactions and persistent dependencies in sequential data such as time series data or signals. GLFormer differs from Transformer and many of its derivatives in that it requires fewer parameters and its computational complexity is linear versus the quadratic computational complexity of Transformer. GLFormer divides the input signals into shorter sequences or patches, embeds the patches into a token sequence via an embedding layer, and extracts SEI features using the combination of a gated attention unit and sliding local self-attention mechanism. The authors collect signals emitted by fifty maritime vessels' Automatic Identification Systems (AIS) and extract the signals' transient and steady-state portions. The authors compare their GLFormer-based SEI approach to four and three alternative SEI and Transformer-based approaches, respectively. The four SEI approaches are Square Integral Bispectrum (SIB) with Support Vector Machines (SVM), Bi-LSTM, a modified version of ResNet [164,178], and InceptionTime [179]. While the conventional Transformer from [177] is used along with the Swin-Transformer [180], and Convolutions to Vision Transformers (CvT) [181] as alternatives to GLFormer. In terms of average percent correct classification performance, the authors' GLFormer-based SEI approach proves superior to all alternative approaches with an accuracy of 96.3% when extracting SEI features from the transient portion of the AIS signals and is second only to Inception-based SEI when using the AIS signals' steady-state portion (90.1% versus 89.4%). However, the real advantage of the GLFormer-based SEI approach is the computational complexity reduction it provides. The authors measure computational complexity in terms of millions of FLOPS and GLFormer requires the fewest FLOPS. For transient-based SEI, GLFormer requires 33 Mega-FLOPS, which is twenty-five Mega-FLOPS lower than the next fewest of the Swin-Transformer-based SEI approach. GLFormer requires sixty-six Mega-FLOPS when performing SEI using the AIS signals' stead-state portion, which is 1,735 Mega-FLOPS lower than the Inception-based SEI approach (highest SEI performance) and fifty Mega-FLOPS lower than the Swin-Transformer-based approach. GLFormer's computational complexity reduction makes it attractive for IoT deployments; especially, if re-training or transfer learning can be performed via cloud, edge, or fog computing resources. Despite its advantages, the authors do not assess GLFormer-based SEI under degrading noise or channel conditions but do state that future work will investigate GLFormer's performance under degrading SNR conditions. Such a study is necessary to ensure GLFormer is a viable SEI approach.

In [182] the authors present a Mahalanobis distance and Chi-squared distribution RF fingerprinting approach focused on providing SEI-based authentication within 5G IoT next-generation networks. The authors show that their approach requires lower training times and fewer resources than five other SEI approaches while achieving a higher average accuracy. The five alternate SEI approaches include traditional and DL-based techniques that include Multiple Discriminant Analysis/Maximum Likelihood (MDA/ML), SVM, *k*-Nearest Neighbors (*k*NN), LSTM, and a multi-sample CNN. Additionally, the authors test their approach on an open-source, 5G management and orchestration stack using cloud computing. The authors make use of a simulated signal set–generated using MATLAB$^{®}$'s Wireless Waveform Generator toolbox–comprised of up to 450 emitters with 100 signals per emitter. The simulated SEI features consist of CFO, amplitude mismatch on the IQ components, phase offset on the IQ components, clock skew, and DC offset. SEI performance is assessed using as few as three to as many as seven of these features; however, results for only CFO, amplitude mismatch, and phase offset are provided. The authors' Mahalanobis distance and Chi-squared distribution RF fingerprinting approach achieves the highest average percent correct classification performance of 99.35% with the poorest performance of 95% being generated by the MDA/ML-based SEI approach. The authors also assess their SEI approach under degrading SNR from 30 dB down to 15 dB and as the number of emitters increases from 50 to 450. Overall, the average percent correct classification performance remains consistent as the number of emitters increases but is negatively impacted by lower SNR values. The average percent correct classification performance is between 92% and 94% at an SNR of 15 dB, which is on average 4% lower than the 20 dB results regardless of the number of emitters. It would have been beneficial to see individual emitter percent correct classification performance because it would have shown cases of confusion between multiple emitters. The authors assert that their approach is intended to authenticate legitimate emitters and detect illegitimate emitters but do not provide any results supporting the latter claim. This is important because the authors use CFO as an emitter identifying feature and CFO is vulnerable to exploitation by adversaries (see Section 4), thus further research should investigate the viability of authenticating legitimate and detecting illegitimate emitters when the CFO is not used as an emitter identifying feature. The authors state that future work will consider alternate channel conditions and signals collected from real IoT emitters.

The papers reviewed in this section employ a variety of techniques and approaches to reduce the computational and resource requirements associated with SEI in an attempt to make it a viable IoT security approach. Most of them focus on reducing the training time and complexity; however, SEI training–at least the initial–can be performed offline where training times and computational resource constraints are less of a factor. Such an approach can be advantageous and trained models updated by either repeating the offline, training process as new signals or data become available or through the use of transfer learning. A few of these papers did explore the use of Edge, Fog, and Cloud computing, which is important as 5G and next-generation networks are deployed and such computing resources are integrated to facilitate network operation and management. Future SEI research needs to consider the challenges associated with transferring and integrating the trained SEI model(s) within IoT devices. For instance, will the SEI model reside on the individual, edge IoT devices or at a central location such as an access point, base station, or a purpose-built device tasked with monitoring a specific portion of the IoT infrastructure? Such considerations will impact how an SEI model is communicated to the employing device; especially, in cases where the edge device lies dormant for long periods and communicates when only necessary to preserve or extend battery life. Communication of an SEI model will add network overhead, which adds complexity. Lastly, the SEI model employing device(s) will need to store the trained model, which will not only increase usage of limited onboard memory but the weights, biases, or other model values will more than likely be quantized. This will impact the SEI model's accuracy, thus future SEI work will need to consider the extent of this impact and how to compensate for it.

7.2. Receiver-Agnostic SEI

Despite the amount of SEI research conducted over the past twenty-five-plus years, the attention paid to "receiver-agnostic" SEI has been limited to a handful of publications [178,183–187]. This is attributed to the fact that SEI research has primarily focused on investigating or developing novel signal representations, feature generation approaches, feature selection techniques, machine learning algorithms, communications standards, or a combination thereof, thus only a single receiver is employed and its unintentional features have little to no impact on the SEI process because they are consistent across all of its received signals. However, when considering large IoT deployments in which devices change base stations or access points due to mobility or entering, leaving, and re-entering the network, then the use of a single receiver is no longer feasible to ensure effective SEI-based security. Such scenarios create the need for an SEI process–built on a single model or trained NN–to be distributed throughout the IoT infrastructure to reduce complexity and simplify development, deployment, and updates in much the same way Tesla® updates the Artificial Intelligence (AI) of its cars [188,189]. This creates a situation in which the receiver collecting signals for the deployed SEI process differs from that used to train it. Since each receiver's RF front end is comprised of its own set of components, sub-systems, and systems, then each will impart its own set of unintentional features that differ from those of the receiver used to collect the training signal set. This mismatch between receivers' features leads to poor SEI performance even when the only change is the use of another receiver [183], thus effective SEI-based IoT security can benefit from a process or processes that train it to learn a set of signal features that are independent of the receiver used in the signal collection. The result is commonly referred to as "receiver-agnostic" SEI. This section summarizes works that investigate receiver-agnostic SEI.

The earliest receiver-agnostic SEI investigation is presented in [183]. The authors of [183] adopt a calibration-based approach to achieve receiver-agnostic SEI. Calibration is facilitated by training a Residual Neural Network (RNN) using a set of "golden" receiver-collected signals. The trained RNN is used to manipulate or change receiver-specific features in another receiver's collected signals to match those present in the golden receiver's collected signals. The authors consider ten receivers that span a range of capabilities from a high-end signal and spectrum analyzer down to mid-range SDRs, which provides a broad assessment of the presented approach to receiver-agnostic SEI. Each receiver is used to collect signals transmitted by twenty-five ZigBee emitters. The authors compare their approach to the simple case of using an augmented signal set to train the SEI process. This augmented signal set is constructed using signals collected by multiple receivers. The authors' calibration-based approach achieves superior receiver-agnostic SEI performance compared to this simple case. The authors also assess their calibration-based approach when the signals are collected by $[1, 2, 3, \ldots 9]$ receiver(s) and under degrading SNR conditions. The result is improved SEI performance when using multiple receivers. The authors only use the high-end spectrum analyzer as the golden receiver, so it is unclear if similar receiver-agnostic SEI performance can be achieved when the golden receiver is a lower-end–in terms of SWaP-C–receiver. Such an investigation can serve to determine the minimum cost needed for implementation by IoT device manufacturers or IoT infrastructure/network administrators. Lastly, the authors do not consider the presence of an RFF-mimicking adversary (see Section 4). The RNN's "re-coloring" nature may increase the similarity between an adversary's mimicked signal features and those present in the original/targeted (a.k.a., the one being mimicked) emitter's signals, thus increasing attack success.

The authors of [184] investigate mitigation of receiver-specific unintentional signal features using a cooperative approach. The authors consider an SEI process tasked with identifying $N_e = 5$ emitters using signals collected by $N_R = 3$ receivers under the assumption that only a single, unknown emitter is operating at the time all receivers are collecting its signals. The authors decompose the received signals using Empirical Mode Decomposition (EMD), Variational Mode Decomposition (VMD), or Intrinsic Time-scale Decomposition (ITD), which is followed by calculation of the skewness and kurtosis of the decomposed signals. SEI is performed using Support Vector Machines (SVM), a Back Propagation (BP) Neural Network (NN), and a Long Short-Term Memory (LSTM) NN. The authors train an SVM for each known receiver (i.e., there a N_R SVMs) and identify the emitters using a "maximum wins" voting process while the single BP-NN and LSTM are trained using the signals collected by all N_R receivers. Thus, the latter two classifiers are trained to learn features that enable receiver-agnostic SEI. The LSTM using skewness and kurtosis calculated from the ITD decomposed signals achieves the highest average accuracy. The authors do not provide individual emitter performance. Also, the authors simulate the emitters' and receivers' effects on ideal signals. The emitter effects considered

doi:10.20944/preprints202307.1165.v1

are IQ imbalance, a spurious tone & carrier leakage, and the power amplifier's non-linear distortion. For the receiver, the authors simulate phase noise, quantization noise, and sampling jitter. Although this approach is good for proof-of-concept demonstration, it is of limited practicality in real-world IoT deployments because emitter features have been shown to change from one transmission to another during normal operation [49]. Additionally, the authors did not investigate cases in which the signals collected by one or more receivers are not available to the SEI process due to conditions that would stimulate re-transmission, a common occurrence in wireless communications. IoT deployments can form Wireless Ad hoc NETworks (WANETs) and Mobile Ad hoc NETworks (MANETs), thus the number of emitters may be equal to or less than the number of receivers. How these topologies impact receiver-agnostic SEI remains an open research question.

In [185], the authors present a Separated Batch Normalization-Deep Adversarial Neural Network (SepBN-DANN) for receiver-agnostic SEI. The authors consider the case when the receiver used to collect the training signals is different than the one used to collect the testing signals, thus the approach in [185] only considers a two-receiver case. The receivers are not specified but are stated to be of the same manufacturer and model. The two-receiver case serves as the impetus behind the authors' use of SepBN because the distributions of the receiver-specific features are not identical across their signal sets. Each receiver's collected signals are used as the training set while the other receiver's signals serve as the testing set. In addition to the use of two receivers, the authors collect the signals of twenty, unspecified emitters over a three-day period. Although they collect signals over multiple days, it does not appear that the authors perform cross-collection (a.k.a., multi-day) SEI (see Section 5.2). The fact that the authors do not provide emitter specifics makes it impossible to determine if the emitters are of the same manufacturer, model, or some combination of manufacturers and models. Such information would indicate the SEI difficulty level because serial number discrimination (a.k.a., all emitters are of the same manufacturer and model) remains the most challenging SEI case. Despite this, the authors show that their SepBN-DANN approach can achieve average SEI accuracies of 90% or higher for each of the three days and regardless of which receiver's signals are used for training. The overall average SEI accuracy–computed across days and receiver used to collect the training signals–is 95.03% for SepBN-DANN versus 90.18% when using only the DANN and 68.22% when using a CNN. The authors do not provide individual emitter accuracy, the specifics of the signal collection setup (e.g., wired connection, wireless, in an anechoic chamber, etc.), or the SNR of the signals and resulting SEI performance. The use of two receivers can initially appear to be a limiting factor but not if the training receiver is considered the "golden" receiver and the testing receiver the deployed IoT device performing SEI, thus providing an opportunity for receiver-agnostic SEI in WANET and MANET configured IoT deployments.

The work in [178] achieves receiver-agnostic SEI by compiling a large data set whose contents include the authorized emitters' signals collected by all receivers. A total of ten LoRa nodes are used as authorized emitters and twenty SDRs as receivers. The set of receivers consists of two USRP N210s, two USRP B210s, two USRP B200s, two USRP B210 Minis, two ADALM Pluto SDRs, and nine RTL-SDR receivers, thus the receivers span a wide range of SWaP-C requirements. The authors' approach to receiver-agnostic SEI uses an adversarial training architecture comprised of a feature extractor and two classifiers. One classifier is tasked with authorized emitter identification and the other with receiver classification. Each signal undergoes CFO correction and normalization to unit energy. Following CFO correction and energy normalization, data augmentation is conducted in accordance with [190]. Data augmentation is applied to the training signals and achieved by passing each of them through a simulated multipath channel with Doppler effects to improve the feature extractor's and both classifiers' robustness to a range of conditions that can be present within an operating environment. Every training and testing signal is then represented using its spectrogram [190]. The authors assess their receiver-agnostic SEI approach under various configurations and conditions to include the number of receivers represented in the training signal set, SNR, homogeneous and heterogeneous receiver configurations within and across the training and testing signal sets, and a six-emitter operational wireless network set up within an office environment without Line-of-Sight (LoS) between the emitters and any of the three receivers. The greatest receiver-agnostic SEI success is achieved using a collaborative approach in which the emitter identity predictions of multiple receivers are combined to form a "fused" prediction. The authors note that SEI accuracy increases as the number of predictions being fused increases. Despite the encouraging results presented in [178], the authors only present average accuracy results, thus there is no way to know how well their approach identifies individual emitters. Overall, the construction of a large signal set that spans all receivers is not an issue so long as the receivers do not change (e.g., replaced) and are known before training the SEI process. However, this may not be practical in operational IoT infrastructures because every new receiver deployment would necessitate the collection of large signal data sets and computationally expensive retraining. Another observation is that the best receiver-agnostic SEI performance occurs when the training and testing receivers are of the same manufacturer and model (e.g., only N210s are used) or when the training receivers are of higher SWaP-C than those used for testing. An example of the latter is when training is conducted using signals collected by the N210s and B210s but the testing signals are collected using the RTL-SDR receivers. Lastly, it is unclear how the approach–presented by the authors of [178]–would fair or be implemented in a WANET or MANET-configured IoT deployment because such configurations face even stricter onboard limitations (e.g., memory, power, computation) and the receivers can and more than likely would change location(s) within a given portion of the network, thus changing the authorized emitter signals that can be collected by a given receiver at any point in time. As previously noted, the latter would require the collection of large signal data sets and the retraining of the affected feature extractors and classifiers.

The authors of [186] investigate two approaches for achieving receiver-agnostic SEI. The authors designate these two approaches as Statistical Distance-based Receiver Agnostic (SD-RXA) and GAN-RXA. Both are trained with the goal of training a feature extractor that extracts receiver-agnostic features from the signals of a set of emitters regardless of the receiver used to collect them. SD-RXA is built on the assumption that the receiver- and emitter-specific features are uncorrelated due to asymmetry between their features and random receiver-emitter pairing. However, the authors conclude the SD-RXA is difficult to work with due to the statistical distance between receiver and emitter feature distributions being nontrivial and tricky, the challenge of selecting an appropriate distance between two distributions, and most importantly the feature extractor's effectiveness in achieving receiver-agnostic SEI cannot be evaluated during training. The GAN-inspired GAN-RXA approach overcomes these difficulties and achieves an average percent correct classification performance of 68% when the GAN-RXA feature extractor is trained using forty emitters and twenty-five receivers and tested using ten emitters and one receiver. This is relatively poor when considering the preponderance of SEI works that achieve average percent correct classification performances of 90% and higher. There may be reasons for this performance disparity. First, the emitters and receivers used for training are mutually exclusive to those used for testing (i.e., no emitter or receiver is used for training and testing). This is important because the feature extractor-learned features will be heavily influenced by the features present in the signals of the training emitters. Although the testing emitters can be of the same manufacturer and model (a.k.a., they only differ in serial number), there are still differences between each emitter's signal features. The impact of these differences is not investigated by the authors of [186]. Second, they use a portion of the publicly available data set provided by the authors of [161], which includes signals collected over multiple days. This is important because SEI performance has been shown to suffer when training and testing are conducted using signals collected at different times (e.g., across multiple days) even when a single receiver is used (see Section 5.2). This makes it difficult to determine if the poor performance is due to the GAN-RXA approach's inability to learn receiver-agnostic SEI features, issues surrounding cross-collection (a.k.a., multi-day) SEI, or a combination of the two. Lastly, the authors do not remove CFO from the signals and are unclear as to whether signal energy is normalized to unity. The presence of either or both may be biasing SEI performance–positively or negatively–and make the presented approach susceptible to adversary exploitation (see Section 4).

The authors of [187] aim to achieve receiver-agnostic SEI by treating the features of the different receivers as a data augmentation technique to train a simple Siamese model using unsupervised learning [191]. The simple Siamese model is then optimized using Local Maximum Mean Discrepancy (LMMD) regularization [192] to capture emitter-specific SEI features. The authors' receiver-agnostic SEI approach achieves an average accuracy of 95% at an unspecified SNR. It is important to note that the authors primarily use simulated emitter and receiver SEI features, but do evaluate their approach using two USRP X310s as the receivers and four USRP N210 emitters. This is a very limited case and not indicative of a realistic IoT deployment that will be comprised of tens to hundreds of devices that are not constructed using high-end (a.k.a., costing more than $3,000 to $15,500 per unit) SDRs. It is also unclear which results correspond to the simulated emitters and receivers versus the SDR-based evaluation. Many of the presented results show three or more receivers, which indicates the simulated emitters and receivers are used. The use of simulated SEI features is a valid approach but clearly pairing them with actual hardware-based results is essential to determining the value of any SEI-focused contribution.

A truly receiver-agnostic SEI process needs to be able to accept signals collected from receivers that were not present during the SEI training process. Also, all of these approaches assume the solution rests in the development of more sophisticated DL algorithms. Although the interest in DL is well-founded and warranted, it may not be the best approach, thus future work needs to look into alternative approaches that are not as demanding in terms of computation, memory, time, and resources to make receiver-agnostic SEI better suited for IoT deployments.

8. Supplemental Challenges

This section highlights key challenges facing SEI that are not already addressed in the previous sections. Some of these challenges must be addressed to move SEI from a proof-of-concept demonstration to a viable, operational security approach capable of protecting IoT deployments.

8.1. Quantization of Deep Learning Models

The demand for less computationally complex, low latency, and high privacy DL algorithms–that can be implemented on edge computing devices such as IoT–is increasing. A primary challenge facing DL model deployment is that they are large in size and require large-scale computation resources that are not available in IoT devices [193]. Specifically, the DNN memory cost prevents them from being directly placed into deployed IoT devices. One way to facilitate DL model deployment on IoT devices with limited storage resources is to use low-bit quantization to approximate or convert full precision (e.g., 32-bit float) NN weights and biases to low-bit representations such as 8-bit integers. The following research efforts are current examples of applying quantization to DL models to facilitate their integration into embedded systems and IoT devices.

- The authors of [194] present a flexible open-source mixed low-precision library referred to as CMix-NN for low-bit quantization of weights and activations into 8-, 4-, and 2-bit integers. The proposed quantization method targets micro-controller units with a few megabytes of memory and without hardware support for floating-point operations. The quantization library can be used to convert convolutional kernels of CNNs to any bit precision in the set of 8-, 4-, and 2-bits. The authors of [194] used the CMix-NN library to compress, deploy, and evaluate the performance of multiple Mobile-net family models on an STM32H7 microcontroller. The CMix-NN library achieves up to an 8% improvement in accuracy compared to the other state-of-the-art quantization and compression solutions for microcontroller units.
- The authors of [195] present effective quantization approaches for Recurrent Neural Network (RNN) implementations that includes LSTM, Gated Recurrent Units (GRU), and Convolutional Long-Short Term Memory (ConvLSTM). The proposed quantization methods are intended for

FPGAs and embedded devices such as low-power mobile devices. The authors of [195] evaluated the performance of their quantization approach using the IMDb and moving MNIST data sets.

Recent SEI research focuses on applying DL for the effective extraction of inherent and discriminating features from the signals' raw IQ samples or their multi-dimensional representations. Although DL has demonstrated success in identifying emitters using learned SEI features, the training of large DL models is a computationally complex process that requires more resources than those available to IoT devices.

The authors of [196] assess SEI performance in the presence of adversarial replay attacks that is demonstrated using an IEEE 802.11a Wi-Fi network comprised of:

- **Access Point (AP)**: provides traditional AP functionality as well as SEI. The AP is powered by a Raspberry Pi 4 model B.
- **Authorized Users**: Each authorized user is a TP-Link AC1300 USB Wi-Fi adapter and a computer running Ubuntu Linux 16.0.
- **Adversary**: The adversary is implemented using an Ettus USRP B210 SDR powered by an NVIDIA Jetson Nano Developer Kit. The adversary actively learns the SEI features of an authorized emitter and then modifies its own signals' SEI features to match those of the selected authorized emitter before transmission in an attempt to hinder or defeat the AP co-located SEI process.

The adversary uses a GAN to learn and mimic the SEI features of an authorized emitter. Initially, the GAN is trained using backpropagation on an NVIDIA Tesla K40m GPU. The adversary's edge computing device–given by the Jetson Nano Developer Kit–has limited storage and computational capability, thus the authors reduced the GAN's trained generator weight and bias values to 12-bit floats via low-bit quantization. This low-bit quantization allowed the authors of [196] to integrate the original model into a limited memory edge computing device. Despite the contributions of the work in [196], it did not assess quantization's impact on the effectiveness or success of the adversary's SEI mimicry countermeasure/attack.

8.2. Unlocking the Secrets of SEI

The inspiration behind SEI is often attributed to human biometrics such as facial recognition, retinal scanning, and fingerprints. The last is the impetus behind SEI's moniker of RF fingerprinting because in SEI the unintentional signal features serve as the "fingerprint" through which a specific emitter is identified. This is based upon the assumption that every emitter's signal features are sufficiently universal, unique, permanent, and collectible. However, this survey summarizes many SEI works that call into question the uniqueness (see Section 4) and permanence (see Section 5.2) of an emitter's unintentional signal features (a.k.a., its fingerprint). Various SEI publications have expressed RF fingerprints similarly to that of Equation (1). Although Equation (1) models unique and unintentional behaviors that manifest in an emitter's transmitted signal; it does not capture the specific mechanism or mechanisms that form them. In other words, Equation (1) assumes a collective approach in which the cumulative effects of an RF front end's components, sub-systems, and systems are "lumped" together into a few parameters, $\Delta A(t)$, Δf, and $\Delta\phi(t)$. This "lumped" approach not only seems to be an oversimplification of the RF front end but could also be the reason SEI's premise of uniqueness and permanence is being challenged. This is because Equation (1) and other similar models may not provide sufficient feature variability to account for the RF front end's complex architecture. This is very important when considering the security of large IoT device populations in which SEI uniqueness and permanence are essential to uniquely and consistently identifying any number of emitters, which the authors of [153] support by noting that DL-based SEI accuracy drops as the number of emitters being identified increases. In comparison, we know that every human–that has ever lived or will live–has a set of fingerprints that are unique and permanent (barring damage that destroys or obscures them). Such an assertion is possible because researchers have determined the mechanism that forms them [197]. However, the mechanism or mechanisms responsible for RF fingerprint formation remain unknown and unexplored but knowing them is essential in determining SEI's viability as an IoT security approach. Thus, further research is needed to unlock the origins of a particular SEI feature or set of features. For instance, what circuits or components within an RF front-end subsystem or system lead to the variability measured within the collected signals? Is that variability sufficient to provide the same level of identification certainty that exists with human fingerprints? The answers to these questions and many others are key to establishing SEI as a viable security solution within an IoT population consisting of millions of devices.

8.3. Availability and Format of Large signal Data Sets

Section 6 provided a summary of four, publicly available signal sets that can and have been used for SEI. As previously noted, these signal sets are constructed using signals transmitted by SDRs, which do not reflect the typical emitters one would expect in low-cost ($30 or less) IoT devices and deployments. Therefore, there is a need for the creation, curation, and dissemination of SEI signal sets that are constructed using COTS emitters. These data sets need to span the wide range of IoT-designated communications standards which include but are not limited to IEEE 802.11 Wi-Fi, LTE, Bluetooth, BLE, ZigBee, LoRa, and SigFox [198], should be collected at the highest sampling frequencies possible, contain the entirety of each transmitted signal, contain channel-only portions to facilitate SNR calculation and other channel-dependent pre-processing and represent tens to hundreds and if possible over 1,000 individual emitters from a variety of manufacturers and models while ensuring that serial number SEI can be performed. Of course, this is assuming that the requisite metadata is included to include receiver specifications, operating bandwidth, center frequency or frequencies, collection settings to include connection type: over-the-air, anechoic, or wired connection, antennas used with their specifications, and collection location (e.g., indoor, outdoor). Lastly, data format and encoding should be done using a known standard and with the highest precision feasible to maximize the preservation of as many SEI features as possible.

8.4. Standardization of Language

The authors of [89] are the first to attempt to tackle this SEI challenge; however, since the publication of [89], this still remains an open challenge/issue. Although the language used within the SEI community is not a technical challenge preventing SEI's transition from a proof-of-concept demonstration to an effective and robust PHY layer-based security solution used within operational IoT deployments, the lack of language commonality can and does hinder clear communication of an SEI work's focus or purpose, how that work relates to the wider community, and outside the community. So, we reiterate the standard language put forward in [89] and encourage researchers to adopt these definitions in their current and future publications.

- <u>Classification:</u> (a.k.a., Identification) The process through which emitters are assigned to different classes or categories. Classification is the result of a *one-to-many* comparison between the emitter's signal or its representation and each of the known classes or categories using a measure of similarity (e.g., distance, probability, etc.).
- <u>Authentication:</u> (a.k.a., Verification or Validation) The process through which an emitter's identity–typically a digital one such as a MAC address–is authenticated or verified by performing a *one-to-one* comparison between the emitter's signal or its representation and the stored model or representation associated with the identity claimed by the to-be-authenticated emitter.

8.5. IoT-imposed Temperature Considerations

It is important to note that all emitters undergo some form of temperature change–typically an increase–as they turn on and begin transmitting until some steady-state operating temperature is reached. This "warming up" period is rather short in duration but SEI features may change over this period. The typical mitigation strategy to alleviate this temperature-dependent feature variation is to allow the to-be-identified emitter to transmit for some set period of time (e.g., five to ten minutes) before performing signal collection or SEI. However, many IoT devices enter a “sleep” or “shutdown” state to preserve or extend battery life and turn on only to transmit their data before returning to “sleep”. This is an important IoT-imposed operational constraint that SEI has yet to but must contend with because this period of activity may be too short in duration to allow the IoT device’s RF front end sufficient time to reach its steady operating temperature conditions. Future IoT-focused SEI investigations need to explore signal feature variation impacts related to this IoT-imposed operating condition.

9. Conclusions

This survey reviewed publications from the perspective of employing SEI as a practical and usable PHY layer-based IoT security mechanism. The number of IoT deployments continues to grow with the total population expected to reach seventy-five billion by 2025. This growth is alarming because it creates an increasing attack surface over which bad actors do and will continue to exploit individual or sets of IoT devices and IoT-connected critical infrastructure. This alarming fact is exacerbated by the knowledge that a majority–70% or more–of IoT devices use weak or no encryption at all due to limited on-board resources such as memory and power, manufacturing costs that are too high to justify the use of encryption, and challenges associated with deploying, implementing, and managing encryption at scale. Due to these security concerns and challenges, SEI has been put forward as a PHY layer means by which to secure IoT devices and their corresponding infrastructure. SEI is advantageous because it is a passive technique that has been shown capable of identifying emitters–down to the serial number–using distinct, inherent, and unintentional features imparted upon their emitted waveforms by the circuits, sub-systems, and systems that comprise their RF front ends. Another justification for an SEI-based IoT security solution is that SEI does not require modification, interrogation, or insertion of additional functionality or capability into the IoT device being identified. This makes SEI ideally suited because it is backward compatible with existing, deployed, and legacy devices without increasing the computational and resource requirements of the end IoT device(s). SEI has been around for almost thirty years with a significant amount of interest focused on it within the past five to eight years; especially, with the emergence of powerful and successful DL algorithms within the facial recognition as well as image and natural language processing communities. Despite the increased attention and the push to deploy SEI as an IoT security solution, it has remained largely the focus of academic efforts. In an effort to change this, we examined SEI works from the perspective of employing SEI as a practical, effective, and usable IoT security approach. In particular, we examined existing SEI works through the lens of SEI’s integration and use in resource-constrained IoT devices, thus we considered works that addressed the impact of the wireless environments channel and temperature, the presence of emitters that actively attempt to obscure or modify their emitter-specific features in an attempt to hinder or defeat an SEI process, the performance of SEI as the number of emitters increased or across multiple collections, the existence of publicly available data sets, the resource limitations of the end IoT devices, and the extraction of receiver-agnostic SEI features. Additionally, this survey considered additional challenges that have not received as much attention within the SEI literature but still hinder SEI’s deployment as an IoT security mechanism. This survey differs from previous SEI surveys in that an IoT-centric perspective was assumed when analyzing the SEI literature.

Author Contributions: Conceptualization, D.R.R.; Survey Structure and Content, D.R.R., J.H.T., and M.K.M.F.; Project administration, D.R.R.; Resources, D.R.R.; Supervision, D.R.R.; Graphic Visualization, J.H.T., and D.R.R.; Writing—original draft, D.R.R., J.H.T., and M.K.M.F.; Writing—review and editing, D.R.R.; All authors have read and agreed to the published version of the manuscript.

Funding: The work presented in this article is supported in part by the Tennessee Higher Education Commission (THEC) through the Center of Excellence in Applied Computational Science and Engineering (CEACSE).

Acknowledgments: The views, analysis, and conclusions presented in this article are those of the authors and should not be interpreted or construed as representing the official policies–expressed or implied–of the Tennessee Higher Education Commission (THEC) or the Center of Excellence in Applied Computational Science and Engineering (CEACSE).

Conflicts of Interest: The authors declare no conflict of interest.

Abbreviations

The following abbreviations are used in this manuscript:

5G	Fifth Generation
5G-NR	Fifth Generation-New Radio
ABL	Adaptive Broad Learning
ADA	Adversarial Domain Adaption
ADLM	Analog Devices Active Learning Module
ADS-B	Automatic Dependent Surveillance-Broadcast
AE	AutoEncoder
AI	Artificial Intelligence
AIS	Automatic Identification System
AM	Amplitude Modulation
AP	Access Point
APG	Average Path Gain
ASCII	American Standard Code for Information Interchange
ASK	Amplitude Shift-Keying
AWG	Arbitrary Waveform Generator
AWGN	Additive White Gaussian Noise
BER	Bit-Error-Rate
BLE	Bluetooth Low Energy
BLS	Broad Learning System
BP	Back Propagation
BPSK	Binary Phase Shift-Keying
BS	Base Station
CAE	Convolutional AutoEncoder
CFO	Carrier Frequency Offset
ChaRRNets	Channel Robust Representation Networks
CGAN	Conditional Generative Adversarial Network
CNN	Convolutional Neural Network
ConvLSTM	Convolutional Long Short-Term Memory
COTS	Commercial-Off-The-Shelf
CPFSK	Continuous-Phase Frequency-Shift Keying
CPU	Central Processing Unit
CSI	Channel State Information
CuSI	Cubic-Spline Interpolation
CvT	Convolutions to Vision Transformers
C&W	Carlini & Wagner
DAC	Digital-to-Analog Converter
DCFT	Differential Constellation Trace Figure
DCT	Discrete Cosine Transform
DDoS	Distributed Denial-of-Service
DFT	Discrete Fourier Transform
DI	Differential Interval
DNA	Distinct, Native, Attribute
DNN	Deep Neural Network
DoLoS	Difference of the Logarithm of the Spectrum
DSB	Double Side-Band
EMD	Empirical Mode Decomposition
FAR	False Accept Rate
FGSM	Fast Gradient Sign Method
FLOPS	Floating Point Operations Per Second
FM	Frequency Modulation
FPGA	Field Programmable Gate Array
FRR	False Reject Rate
GAN	Generative Adversarial Network
GAN-RXA	Generative Adversarial Network-based Receiver Agnostic
GFSK	Gaussian Frequency-Shift Keying
GLFormer	Gated and sliding Local self-attention transFormer
GMSK	Gaussian Minimum Shift-Keying

GPU	Graphical Processing Unit
GRU	Gated Recurrent Unit
GT	Gabor Transform
HART	Highway Addressable Remote Transducer
ICMP	Internet Control Message Protocol
IIR	Infinite Impulse Response
InfoGANs	Information maximized Generative Adversarial Networks
IoT	Internet of Things
IoV	Internet of Vehicles
IoBT	Internet of Battlefield Things
IoMT	Internet of Military Things
IIoT	Industrial Internet of Things
IQ	In-phase & Quadrature
IQI	IQ Imbalance
ISM	Industrial, Scientific, and Medical
ISR	Intentional Structure Removal
ITD	Intrinsic Time-scale Decomposition
JCAECNN	Joint CAE and CNN
*k*NN	*k*-Nearest Neighbors
LAI	Linear Approximation Interpolation
LMMD	Local Maximum Mean Discrepancy
LO	Local Oscillator
LoS	Line-of-Sight
LSTM	Long Short-Term Memory
LTE	Long-Term Evolution
LTS	Long Training Symbol
MAC	Media Access Control
MANET	Mobile Ad hoc NETwork
MDA	Multiple Discriminant Analysis
MDA/ML	Multiple Discriminant Analysis/Maximum Likelihood
MIMO	Multiple Input Multiple Output
MLP	Multi-Layer Perceptron
MMSE	Minimum Mean Squared Error
N-M	Nelder-Mead
NN	Neural Network
OFDM	Orthogonal Frequency-Division Multiplexing
OOK	On-Off Keying
OQPSK	Offset Quadrature Phase-Shift Keying
ORACLE	Optimized Radio clAssification through Convolutional neuraL nEtworks
ORANs	Open Radio Access Networks
OSTBC	Orthogonal Space-Time Block Code
PA	Power Amplifier
PAM	Pulse Amplitude Modulation
PARADIS	Passive RAdiometric Device Identification System
PBA	Per Batch Accuracy
PCA	Principal Component Analysis
PGD	Projected Gradient Descent
PHY	Physical
PLA	Physical Layer Authentication
PLL	Phase-Locked Loop
PMF	Probability Mass Function
POWDER	Platform for Open Wireless Data-driven Experimental Research
PSA	Per Slice Accuracy
PSK	Phase Shift-Keying
PTA	Per-Transmission Accuracy
QAM	Quadrature Amplitude Modulation
QoS	Quality of Service
QPSK	Quadrature Phase Shift-Keying
RECAP	Radiometric signature Exploitation Countering using Adversarial machine learning-based Protocol
RF	Radio Frequency
RFF	Radio Frequency Fingerprint
RFFE	Radio Frequency Fingerprint Embedding

RF-DNA	Radio Frequency-Distinct, Native, Attributes
RNN	Recurrent Neural Network
SC	Suppressed Carrier
SDR	Software-Defined Radio
SD-RXA	Statistical Distance-based Receiver Agnostic
SEI	Specific Emitter Identification
SepBN-DANN	Separated Batch Normalization-Deep Adversarial Neural Network
SFEBLN	Signal Feature Embedded Broad Learning Network
SIB	Square Integral Bispectrum
SigMF	Signal Metadata Format
SNR	Signal-to-Noise Ratio
STS	Short Training Symbol
STBC	Space-Time Block Code
STFT	Short-Time Fourier Transform
SSB	Single Side-Band
SVM	Support Vector Machines
SWaP-C	Size, Weight, and Power-Cost
SYNC	Synchronization
TeRFF	Temperature-aware Radio Frequency Fingerprinting
TF	Time-Frequency
USRP	Universal Software Radio Peripheral
VCP	Voltage Controlled Oscillator
VMD	Variational Mode Decomposition
WANET	Wireless Ad hoc NETwork
WBFM	Wide-Band Frequency Modulation
WC	Without Carrier
Wi-Fi	Wireless-Fidelity
WLAN	Wireless Local Area Network
ZSL	Zero-Shot Learning

References

1. Department of Defense (DoD), United States. DoD Policy Recommendations for the Internet of Things (IoT). https://www.hsdl.org/?view&did=799676, 2016.
2. Gartner Research. Gartner Says 6.4 Billion Connected"Things" Will Be in Use in 2016, Up 30 Percent From 2015, 2015.
3. Juniper Research. 'Internet of Things' Connected Devices to Triple by 2021, Reaching Over 46 Billion Units, 2016.
4. Statista. Internet of Things (IoT) connected devices installed base worldwide from 2015 to 2025 (in billions). https://www.statista.com/statistics/471264/iot-number-of-connected-devices-worldwide/, 2019.
5. Rawlinson, K. Hp study reveals 70 percent of internet of things devices vulnerable to attack. [Online], https://www8.hp.com/us/en/hp-news/press-release.html?id=1744676, 2014.
6. Ray, I.; Kar, D.M.; Peterson, J.; Goeringer, S. Device identity and trust in IoT-sphere forsaking cryptography. 2019 IEEE 5th International Conference on Collaboration and Internet Computing (CIC). IEEE, 2019, pp. 204–213.
7. Neshenko, N.; Bou-Harb, E.; Crichigno, J.; Kaddoum, G.; Ghani, N. Demystifying IoT security: an exhaustive survey on IoT vulnerabilities and a first empirical look on internet-scale IoT exploitations. *IEEE Communications Surveys & Tutorials* **2019**, *21*, 2702–2733.
8. Larson, S. A smart fish tank left a casino vulnerable to hackers, 2017.
9. Wright, J.; Cache, J. *Hacking exposed wireless: Wireless security secrets & solutions*; McGraw-Hill Education Group, 2015.
10. Stanislav, M.; Beardsley, T. Hacking iot: A case study on baby monitor exposures and vulnerabilities. *Rapid7 Report* **2015**.
11. Wright, J. KillerBee: Practical ZigBee Exploitation Framework or" Wireless Hacking and the Kinetic World", 2018.
12. Shipley, P.; Gooler, R. Insteon: False security and deceptive documentation. *DEF CON* **2015**, *23*.
13. Shipley, P. Tools for Insteon RF. *GitHub* **2015**.
14. Krebs, B. Mirai IoT Botnet Co-Authors Plead Guilty-Krebs on Security. *Krebs on Security.* **2017**.

15. Simon, S.; Selyukh, A. Internet Of Things' Hacking Attack Led To Widespread Outage Of Popular Websites. *National Public Radio (NPR)* **2016**.
16. Talbot, C.M.; Temple, M.A.; Carbino, T.J.; Betances, J.A. Detecting rogue attacks on commercial wireless Insteon home automation systems. *Computers & security* **2018**, *74*, 296–307.
17. Sa, K.; Lang, D.; Wang, C.; Bai, Y. Specific emitter identification techniques for the internet of things. *IEEE Access* **2019**, *8*, 1644–1652.
18. Reising, D.; Cancelleri, J.; Loveless, T.D.; Kandah, F.; Skjellum, A. Radio identity verification-based IoT security using RF-DNA fingerprints and SVM. *IEEE Internet of Things Journal* **2020**, *8*, 8356–8371.
19. Langley, L.E. Specific emitter identification (SEI) and classical parameter fusion technology. Proceedings of WESCON'93. IEEE, 1993, pp. 377–381.
20. Terry, I. Networked Specific Emitter Identification in Fleet Battle Experiment Juliet. [Online], https://apps.dtic.mil/sti/citations/ADA415972, 2003.
21. Defence R&D Canada - Ottawa. Interferometric Intrapulse Radar Receiver for Specific Emitter Identification and Direction-Finding. *Fact Sheet REW 224* **2007**.
22. Dudczyk, J.; Kawalec, A. Specific emitter identification based on graphical representation of the distribution of radar signal parameters. *Bulletin of the Polish Academy of Sciences. Technical Sciences* **2015**, *63*, 391–396.
23. Matuszewski, J. Specific emitter identification. 2008 International Radar Symposium. IEEE, 2008, pp. 1–4.
24. Toonstra, J.; Kinsner, W. Transient analysis and genetic algorithms for classification. IEEE WESCANEX 95. Communications, Power, and Computing. Conference Proceedings. IEEE, 1995, Vol. 2, pp. 432–437.
25. Ureten, O.; Serinken, N. Detection of radio transmitter turn-on transients. *Electronics letters* **1999**, *35*.
26. Ureten, O.; Serinken, N. Bayesian detection of Wi-Fi transmitter RF fingerprints. *Electronics letters* **2005**, *41*, 373–374.
27. Ureten, O.; Serinken, N. Wireless security through RF fingerprinting. *Canadian Journal of Electrical and Computer Engineering* **2007**, *32*, 27–33.
28. Jana, S.; Kasera, S.K. On fast and accurate detection of unauthorized wireless access points using clock skews. Proceedings of the 14th ACM international conference on Mobile computing and networking, 2008, pp. 104–115.
29. Brik, V.; Banerjee, S.; Gruteser, M.; Oh, S. Wireless device identification with radiometric signatures. Proceedings of the 14th ACM international conference on Mobile computing and networking, 2008, pp. 116–127.
30. Suski II, W.C.; Temple, M.A.; Mendenhall, M.J.; Mills, R.F. Radio frequency fingerprinting commercial communication devices to enhance electronic security. *International Journal of Electronic Security and Digital Forensics* **2008**, *1*, 301–322.
31. Suski II, W.C.; Temple, M.A.; Mendenhall, M.J.; Mills, R.F. Using spectral fingerprints to improve wireless network security. IEEE GLOBECOM 2008-2008 IEEE Global Telecommunications Conference. IEEE, 2008, pp. 1–5.
32. Danev, B.; Capkun, S. Transient-based identification of wireless sensor nodes. 2009 International Conference on Information Processing in Sensor Networks. IEEE, 2009, pp. 25–36.
33. Klein, R.; Temple, M.A.; Mendenhall, M.J.; Reising, D.R. Sensitivity analysis of burst detection and RF fingerprinting classification performance. 2009 IEEE International Conference on Communications. IEEE, 2009, pp. 1–5.
34. Klein, R.W.; Temple, M.A.; Mendenhall, M.J. Application of wavelet-based RF fingerprinting to enhance wireless network security. *Journal of Communications and Networks* **2009**, *11*, 544–555.
35. Liu, M.W.; Doherty, J.F. Specific emitter identification using nonlinear device estimation. 2008 IEEE Sarnoff Symposium. IEEE, 2008, pp. 1–5.
36. Liu, M.W.; Doherty, J.F. Nonlinearity estimation for specific emitter identification in multipath channels. *IEEE Transactions on Information Forensics and Security* **2011**, *6*, 1076–1085.
37. Kennedy, I.O.; Kuzminskiy, A.M. RF fingerprint detection in a wireless multipath channel. 2010 7th International Symposium on Wireless Communication Systems. IEEE, 2010, pp. 820–823.
38. Reising, D.R.; Temple, M.A.; Mendenhall, M.J. Improving intra-cellular security using air monitoring with RF fingerprints. 2010 IEEE Wireless Communication and Networking Conference. IEEE, 2010, pp. 1–6.
39. Reising, D.R.; Temple, M.A.; Mendenhall, M.J. Improved wireless security for GMSK-based devices using RF fingerprinting. *International Journal of Electronic Security and Digital Forensics* **2010**, *3*, 41–59.

40. Reising, D., D. Prentice, and M. Temple. An FPGA Implementation of Real-Time RF-DNA Fingerprinting for RFINT Applications. IEEE Military Communications Conference (MILCOM), 2011.
41. Reising, D.R.; Temple, M.A.; Oxley, M.E. Gabor-based RF-DNA fingerprinting for classifying 802.16 e WiMAX mobile subscribers. 2012 International Conference on Computing, Networking and Communications (ICNC). IEEE, 2012, pp. 7–13.
42. Reising, D.R.; Temple, M.A.; Jackson, J.A. Authorized and rogue device discrimination using dimensionally reduced RF-DNA fingerprints. *IEEE Transactions on Information Forensics and Security* **2015**, *10*, 1180–1192.
43. Williams, M.D.; Temple, M.A.; Reising, D.R. Augmenting bit-level network security using physical layer RF-DNA fingerprinting. 2010 IEEE Global Telecommunications Conference GLOBECOM 2010. IEEE, 2010, pp. 1–6.
44. Takahashi, D.; Xiao, Y.; Zhang, Y.; Chatzimisios, P.; Chen, H.H. IEEE 802.11 user fingerprinting and its applications for intrusion detection. *Computers & Mathematics with Applications* **2010**, *60*, 307–318.
45. Tekbaş, Ö.; Üreten, O.; Serinken, N. Improvement of transmitter identification system for low SNR transients. *Electronics Letters* **2004**, *40*, 182–183.
46. Ellis, K.; Serinken, N. Characteristics of radio transmitter fingerprints. *Radio Science* **2001**, *36*, 585–597.
47. Soliman, S.S.; Hsue, S.Z. Signal classification using statistical moments. *IEEE Transactions on Communications* **1992**, *40*, 908–916.
48. Azzouz, E.; Nandi, A.K. *Automatic modulation recognition of communication signals*; Springer Science & Business Media, 2013.
49. Wheeler, C.G.; Reising, D.R. Assessment of the impact of CFO on RF-DNA fingerprint classification performance. 2017 International Conference on Computing, Networking and Communications (ICNC). IEEE, 2017, pp. 110–114.
50. Pan, Y., S. Yang, H. Peng, T. Li, and W. Wang. Specific Emitter Identification Based on Deep Residual Networks. *Access* **2019**. doi:10.1109/ACCESS.2019.2913759.
51. Fadul, M.K.; Reising, D.R.; Loveless, T.D.; Ofoli, A.R. RF-DNA fingerprint classification of OFDM signals using a Rayleigh fading channel model. 2019 IEEE Wireless Communications and Networking Conference (WCNC). IEEE, 2019, pp. 1–7.
52. Fadul, M., D. Reising, T. D. Loveless, and A. Ofoli. Preprint: Using RF-DNA Fingerprints To Classify OFDM Transmitters Under Rayleigh Fading Conditions. *IEEE Trans on Info Forensics & Security* **2020**.
53. Fadul, M., D. Reising, and M. Sartipi. Identification of OFDM-based Radio sunder Rayleigh Fading using RF-DNA and Deep Learning. *Access* **2020, Under Review**.
54. Dubendorfer, C.K.; Ramsey, B.W.; Temple, M.A. An RF-DNA verification process for ZigBee networks. MILCOM 2012-2012 IEEE Military Communications Conference. IEEE, 2012, pp. 1–6.
55. Baldini, G., G. Steri. A Survey of Techniques for the Identification of Mobile Phones Using the Physical Fingerprints of the Built-In Components. *IEEE Communications Surveys & Tutorials* **2017**, *19*, 1761–1789.
56. Baldini, G., C. Gentile, R. Giuliani and G. Steri. Comparison of Techniques for Radiometric Identification based on Deep Convolutional Neural Networks. *Electronics Letters* **2019**, *55*. doi:10.1049/el.2018.6229.
57. Baldini, G. and R. Giuliani. An Assessment of the Impact of Wireless Interferences on IoT Emitter Identification using Time Frequency Representations and CNN. Global IoT Summit (GIoTS), 2019. doi:10.1109/GIOTS.2019.8766385.
58. Restuccia, F.; D'Oro, S.; Al-Shawabka, A.; Belgiovine, M.; Angioloni, L.; Ioannidis, S.; Chowdhury, K.; Melodia, T. DeepRadioID: Real-time channel-resilient optimization of deep learning-based radio fingerprinting algorithms. Proceedings of the Twentieth ACM International Symposium on Mobile Ad Hoc Networking and Computing, 2019, pp. 51–60.
59. Wong, L., W. Headley, S. Andrews, R. Gerdes and A. Michaels. Clustering Learned CNN Features from Raw I/Q Data for Emitter Identification. IEEE Military Communications Conf (MILCOM), 2018. doi:10.1109/MILCOM.2018.8599847.
60. Jafari, H., O. Omotere, D. Adesina, H. Wu, and L. Qian. IoT Devices Fingerprinting Using Deep Learning. IEEE Military Communications Conf (MILCOM), 2018. doi:10.1109/MILCOM.2018.8599826.
61. Bassey, J., X. Li, and L. Qian. Device Authentication Codes based on RF Fingerprinting using Deep Learning. *arXiv, Electrical Engineering and Systems Science, Signal Processing* **2020**.
62. Chen, X.; Hao, X. Feature Reduction Method for Cognition and Classification of IoT Devices Based on Artificial Intelligence. *Access* **2019**, *7*, 103291–103298. doi:10.1109/ACCESS.2019.2929311.

63. O'Shea, T., T. Roy, and T. Clancy. Over-the-Air Deep Learning Based Radio Signal Classification. *IEEE J. of Selected Topics in Signal Processing* **2018**, *12*. doi:10.1109/JSTSP.2018.2797022.
64. Youssef, K., L. Bouchard, K. Haigh, J. Silovsky, B. Thapa, and C. Valk. Machine Learning Approach to RF Transmitter Identification. *IEEE J. of Radio Frequency Identification* **2018**, *2*. doi:10.1109/JRFID.2018.2880457.
65. Wilson, A.J.; Reising, D.R.; Loveless, T.D. Integration of matched filtering within the RF-DNA fingerprinting process. 2019 IEEE Global Communications Conference (GLOBECOM). IEEE, 2019, pp. 1–6.
66. Hall, J.; Barbeau, M.; Kranakis, E.; others. Detection of transient in radio frequency fingerprinting using signal phase. *Wireless and optical communications* **2003**, *9*, 13.
67. Hall, M. Correlation-based Feature Selection for Discrete and Numeric Class Machine Learning. *Proceedings of the 17th international conference on machine learning (ICML-2000)* **2000**, pp. 359–366.
68. Hall, J.; Barbeau, M.; Kranakis, E. Radio frequency fingerprinting for intrusion detection in wireless networks. *IEEE Transactions on Defendable and Secure Computing* **2005**, *12*, 1–35.
69. Merchant, K., S. Revay, G. Stantchev and B. Nousain. Deep Learning for RF Device Fingerprinting in Cognitive Communication Networks. *IEEE J. of Selected Topics in Sig Proc* **2018**, *12*. doi:10.1109/JSTSP.2018.2796446.
70. Polak, A., and D. Goeckel. RF Fingerprinting of Users Who Actively Mask Their Identities with Artificial Distortion. 2011 Conference Record of the Forty Fifth Asilomar Conference on Signals, Systems and Computers (ASILOMAR), 2011.
71. Polak, A., and D. Goeckel. Wireless Device Identification Based on RF Oscillator Imperfections. *IEEE Transactions on Information Forensics and Security* **2015**, *10*.
72. Polak, A., S. Dolatshahi, and D. Goeckel. Identifying Wireless Users via Transmitter Imperfections. *IEEE Journal on Selected Areas in Communications* **2011**, *29*.
73. Polak, A., and D. Goeckel. Identification of Wireless Devices of Users Who Actively Fake Their RF Fingerprints With Artificial Data Distortion. *IEEE Transactions on Wireless Communications* **2015**, *14*.
74. Dolatshahi, S., A. Polak, and D. Goeckel. Identification of wireless users via power amplifier imperfections. 2010 Conference Record of the Forty Fourth Asilomar Conference on Signals, Systems and Computers, 2010.
75. Yu, J., A. Hu, G. Li, and L. Peng. A Robust RF Fingerprinting Approach Using Multisampling Convolutional Neural Network. *IEEE Internet of Things Journal* **2019**, *6*, 6786–6799.
76. Guyue, L., Y. Jiabao, Y. Xing, and A. Hu. Location-Invariant Physical Layer Identification Approach for WiFi Devices. *Access* **2019**. doi:10.1109/ACCESS.2019.2933242.
77. Liang, J., Z. Huang, and Z. Li. Method of Empirical Mode Decomposition in Specific Emitter Identification. *Wireless Personal Communications* **2017**, *96*, 1–15. doi:10.1007/s11277-017-4306-0.
78. Smith, L., N. Smith, J. Hopkins, D. Rayborn, J. Ball, B. Tang, and M. Young. Classifying WiFi Physical Fingerprints using Complex Deep Learning. Automatic Target Recognition XXX. International Society for Optics and Photonics, 2020, Vol. 11394, p. 113940J.
79. Kandah, F., J. Cancelleri, D. Reising, A. Altarawneh, and A. Skjellum. A Hardware-Software Co-design Approach to Identity, Trust, and Resilience for IoT/CPS at Scale. International Conference on Internet of Things (iThings), 2019.
80. Harmer, P.K.; Temple, M.A.; Buckner, M.A.; Farquhar, E. 4G Security Using Physical Layer RF-DNA with DE-Optimized LFS Classification. *J. Commun.* **2011**, *6*, 671–681.
81. Harmer, P.K.; Reising, D.R.; Temple, M.A. Classifier selection for physical layer security augmentation in cognitive radio networks. 2013 IEEE International Conference on Communications (ICC). IEEE, 2013, pp. 2846–2851.
82. Wang, X., P. Hao, and L. Hanzo. Physical-layer Authentication for Wireless Security Enhancement: Current Challenges and Future Developments. *IEEE Communications Magazine* **2016**, *54*, 152–158.
83. Xu, Q.; Zheng, R.; Saad, W.; Han, Z. Device fingerprinting in wireless networks: Challenges and opportunities. *IEEE Communications Surveys & Tutorials* **2015**, *18*, 94–104.
84. Gerdes, R., T. Daniels, M. Phd, and S. Russell. "Device Identification via Analog Signal Fingerprinting: A Matched Filter Approach,". NDSS Symposium, 2006.
85. Joo, K.; Choi, W.; Lee, D.H. Hold the door! fingerprinting your car key to prevent keyless entry car theft. *arXiv preprint arXiv:2003.13251* **2020**.
86. Riyaz, S., K. Sankhe, S. Ioannidis, and K. Chowdhury. Deep Learning Convolutional Neural Networks for Radio Identification. *IEEE Communications Magazine* **2018**, *56*. doi:10.1109/MCOM.2018.1800153.

87. O'Shea, T., and J. Hoydis. An Introduction to Deep Learning for the Physical Layer. *IEEE Trans on Cognitive Communications & Networking* **2017**, *3*. doi:10.1109/TCCN.2017.2758370.
88. Mendis, G., J. Wei, and A. Madanayake. Deep Learning Based Radio-Signal Identification With Hardware Design. *IEEE Trans on Aerospace & Electronic Systems* **2019**, *55*. doi:10.1109/TAES.2019.2891155.
89. Baldini, G.; Steri, G. A survey of techniques for the identification of mobile phones using the physical fingerprints of the built-in components. *IEEE Communications Surveys & Tutorials* **2017**, *19*, 1761–1789.
90. Jain, A.K.; Hong, L.; Pankanti, S.; Bolle, R. An identity-authentication system using fingerprints. *Proceedings of the IEEE* **1997**, *85*, 1365–1388.
91. Bai, L.; Zhu, L.; Liu, J.; Choi, J.; Zhang, W. Physical layer authentication in wireless communication networks: A survey. *Journal of Communications and Information Networks* **2020**, *5*, 237–264.
92. Clarke, R.H. A statistical theory of mobile-radio reception. *Bell system technical journal* **1968**, *47*, 957–1000.
93. Danev, B.; Luecken, H.; Capkun, S.; El Defrawy, K. Attacks on physical-layer identification. Proceedings of the third ACM conference on Wireless network security, 2010, pp. 89–98.
94. Soltanieh, N.; Norouzi, Y.; Yang, Y.; Karmakar, N.C. A Review of Radio Frequency Fingerprinting Techniques. *IEEE Journal of Radio Frequency Identification* **2020**, *4*, 222–233. doi:10.1109/JRFID.2020.2968369.
95. Xie, N.; Li, Z.; Tan, H. A survey of physical-layer authentication in wireless communications. *IEEE Communications Surveys & Tutorials* **2020**, *23*, 282–310.
96. Liu, Y.; Wang, J.; Li, J.; Niu, S.; Song, H. Machine learning for the detection and identification of Internet of Things devices: A survey. *IEEE Internet of Things Journal* **2021**, *9*, 298–320.
97. Wang, N.; Wang, P.; Alipour-Fanid, A.; Jiao, L.; Zeng, K. Physical-layer security of 5G wireless networks for IoT: Challenges and opportunities. *IEEE Internet of Things Journal* **2019**, *6*, 8169–8181.
98. Jagannath, A.; Jagannath, J.; Kumar, P.S.P.V. A comprehensive survey on radio frequency (rf) fingerprinting: Traditional approaches, deep learning, and open challenges. *arXiv preprint arXiv:2201.00680* **2022**.
99. Parmaksiz, H.; Karakuzu, C. A Review of Recent Developments on Secure Authentication Using RF Fingerprints Techniques. *Sakarya University Journal of Computer and Information Sciences* **2022**, *5*, 278–303.
100. Brandes, T.S.; Kuzdeba, S.; McClelland, J.; Bomberger, N.; Radlbeck, A. RF waveform synthesis guided by deep reinforcement learning. 2020 IEEE International Workshop on Information Forensics and Security (WIFS). IEEE, 2020, pp. 1–6.
101. Wang, W.; Gan, L. Radio Frequency Fingerprinting Improved by Statistical Noise Reduction. *IEEE Transactions on Cognitive Communications and Networking* **2022**.
102. Han, H.; Cui, L.; Li, W.; Huang, L.; Cai, Y.; Cai, J.; Zhang, Y. Radio Frequency Fingerprint Based Wireless Transmitter Identification Against Malicious Attacker: An Adversarial Learning Approach. 2020 International Conference on Wireless Communications and Signal Processing (WCSP). IEEE, 2020, pp. 310–315.
103. Yuan, Y.; Huang, Z.; Wu, H.; Wang, X. Specific emitter identification based on Hilbert–Huang transform-based time–frequency–energy distribution features. *IET communications* **2014**, *8*, 2404–2412.
104. Guo, S.; Akhtar, S.; Mella, A. A method for radar model identification using time-domain transient signals. *IEEE Transactions on Aerospace and Electronic Systems* **2021**, *57*, 3132–3149.
105. Chen, N.; Hu, A.; Fu, H. LoRa radio frequency fingerprint identification based on frequency offset characteristics and optimized LoRaWAN access technology. 2021 IEEE 5th Advanced Information Technology, Electronic and Automation Control Conference (IAEAC). IEEE, 2021, Vol. 5, pp. 1801–1807.
106. Gu, X.; Wu, W.; Guo, N.; He, W.; Song, A.; Yang, M.; Ling, Z.; Luo, J. TeRFF: Temperature-aware Radio Frequency Fingerprinting for Smartphones. 2022 19th Annual IEEE International Conference on Sensing, Communication, and Networking (SECON). IEEE, 2022, pp. 127–135.
107. Chen, Y.; Chen, X.; Lei, Y. Emitter Identification of Digital Modulation Transmitter Based on Nonlinearity and Modulation Distortion of Power Amplifier. *Sensors* **2021**, *21*, 4362.
108. Liting, S.; Xiang, W.; Huang, Z. Unintentional modulation evaluation in time domain and frequency domain. *Chinese Journal of Aeronautics* **2022**, *35*, 376–389.
109. Zhang, J., R. Woods, M. Sandell, M. Valkama, A. Marshall, and J. Cavallaro. Radio Frequency Fingerprint Identification for Narrowband Systems, Modelling and Classification. *IEEE Transactions on Information Forensics and Security* **2021**, *16*, 3974–3987. doi:10.1109/TIFS.2021.3088008.

doi:10.20944/preprints202307.1165.v1

110. Brik, V.; Banerjee, S.; Gruteser, M.; Oh, S. Wireless device identification with radiometric signatures. Proceedings of the 14th ACM international conference on Mobile computing and networking, 2008, pp. 116–127.
111. Hou, W.; Wang, X.; Chouinard, J.Y.; Refaey, A. Physical layer authentication for mobile systems with time-varying carrier frequency offsets. *IEEE Transactions on Communications* **2014**, *62*, 1658–1667.
112. Robyns, P.; Marin, E.; Lamotte, W.; Quax, P.; Singelée, D.; Preneel, B. Physical-layer fingerprinting of LoRa devices using supervised and zero-shot learning. Proceedings of the 10th ACM Conference on Security and Privacy in Wireless and Mobile Networks, 2017, pp. 58–63.
113. Hao, P.; Wang, X.; Behnad, A. Relay authentication by exploiting I/Q imbalance in amplify-and-forward system. 2014 IEEE Global Communications Conference. IEEE, 2014, pp. 613–618.
114. Xing, G.; Shen, M.; Liu, H. Frequency offset and I/Q imbalance compensation for direct-conversion receivers. *IEEE Transactions on Wireless Communications* **2005**, *4*, 673–680.
115. Jian, T., B. Rendon, E. Ojuba, N. Soltani, Z. Wang, K. Sankhe, A. Gritsenko, J. Dy, K. Chowdhury, and S. Ioannidis. Deep Learning for RF Fingerprinting: A Massive Experimental Study. *IEEE Internet of Things Magazine* **2020**, *3*, 50–57. doi:10.1109/IOTM.0001.1900065.
116. Robinson, J., S. Kuzdeba, J. Stankowicz, and J. Carmack. Dilated Causal Convolutional Model For RF Fingerprinting. 2020 10th Annual Computing and Communication Workshop and Conference (CCWC), 2020, pp. 0157–0162. doi:10.1109/CCWC47524.2020.9031257.
117. Morin, C.; Cardoso, L.S.; Hoydis, J.; Gorce, J.M.; Vial, T. Transmitter classification with supervised deep learning. Cognitive Radio-Oriented Wireless Networks: 14th EAI International Conference, CrownCom 2019, Poznan, Poland, June 11–12, 2019, Proceedings 14. Springer, 2019, pp. 73–86.
118. Behura, S.; Kedia, S.; Hiremath, S.M.; Patra, S.K. WiST ID—Deep Learning-Based Large Scale Wireless Standard Technology Identification. *IEEE Transactions on Cognitive Communications and Networking* **2020**, *6*, 1365–1377. doi:10.1109/TCCN.2020.2985375.
119. Wang, J.; Zhang, B.; Zhang, J.; Yang, N.; Wei, G.; Guo, D. Specific Emitter Identification Based on Deep Adversarial Domain Adaptation. 2021 4th International Conference on Information Communication and Signal Processing (ICICSP), 2021, pp. 104–109. doi:10.1109/ICICSP54369.2021.9611854.
120. Gong, J.; Xu, X.; Qin, Y.; Dong, W. A Generative Adversarial Network Based Framework for Specific Emitter Characterization and Identification. 2019 11th International Conference on Wireless Communications and Signal Processing (WCSP), 2019, pp. 1–6. doi:10.1109/WCSP.2019.8927888.
121. Gong, J.; Xu, X.; Lei, Y. Unsupervised Specific Emitter Identification Method Using Radio-Frequency Fingerprint Embedded InfoGAN. *IEEE Transactions on Information Forensics and Security* **2020**, *15*, 2898–2913. doi:10.1109/TIFS.2020.2978620.
122. Basha, N.; Hamdaoui, B.; Sivanesan, K.; Guizani, M. Channel-Resilient Deep-Learning-Driven Device Fingerprinting Through Multiple Data Streams. *IEEE Open Journal of the Communications Society* **2023**.
123. Xing, Y.; Hu, A.; Zhang, J.; Peng, L.; Wang, X. Design of A Channel Robust Radio Frequency Fingerprint Identification Scheme. *IEEE Internet of Things Journal* **2022**.
124. Yuan, H.; Yan, Y.; Bao, Z.; Xu, C.; Gu, J.; Wang, J. Multipath Canceled RF Fingerprinting for Wireless OFDM Devices Based on Hammerstein System Parameter Separation. *IEEE Canadian Journal of Electrical and Computer Engineering* **2022**, *45*, 401–408.
125. Yang, L.; Camtepe, S.; Gao, Y.; Liu, V.; Jayalath, D. On the Use of Power Amplifier Nonlinearity Quotient to Improve Radio Frequency Fingerprint Identification in Time-Varying Channels. *arXiv preprint arXiv:2302.13724* **2023**.
126. Fadul, M.; Reising, D.; Loveless, T.D.; Ofoli, A. Nelder-mead simplex channel estimation for the RF-DNA fingerprinting of OFDM transmitters under Rayleigh fading conditions. *IEEE Transactions on Information Forensics and Security* **2021**, *16*, 2381–2396.
127. Reising, D.R.; Weerasena, L.P.; Loveless, T.D.; Sartipi, M.; others. Improving RF-DNA Fingerprinting Performance in an Indoor Multipath Environment Using Semi-Supervised Learning. *arXiv preprint arXiv:2304.00648* **2023**.
128. Brown, C.N.; Mattei, E.; Draganov, A. ChaRRNets: Channel robust representation networks for RF fingerprinting. *arXiv preprint arXiv:2105.03568* **2021**.
129. Tyler, J., M. Fadul, D. Reising, and F. Kandah. An Analysis of Signal Energy Impacts and Threats to Deep Learning Based SEI. IEEE Int'l Conf on Communications (ICC) ACCEPTED, 2022.

130. Rehman, S.; Sowerby, K.; Alam, S.; Ardekani, I. Radio frequency fingerprinting and its challenges. 2014 IEEE conference on communications and network security. IEEE, 2014, pp. 496–497.
131. Wang, T.; Fang, K.; Wei, W.; Tian, J.; Pan, Y.; Li, J. Microcontroller Unit Chip Temperature Fingerprint Informed Machine Learning for IIoT Intrusion Detection. *IEEE Transactions on Industrial Informatics* **2022**, *19*, 2219–2227.
132. Yilmaz, Ö.; Yazici, M. The Effect of Ambient Temperature On Device Classification Based On Radio Frequency Fingerprint Recognition. *Sakarya University Journal of Computer and Information Sciences* **2022**, *5*, 233–245.
133. Frerking, M. *Crystal oscillator design and temperature compensation*; Springer Science & Business Media, 2012.
134. Peggs, C.S.; Jackson, T.S.; Tittlebaugh, A.N.; Olp, T.G.; Tyler, J.H.; Reising, D.R.; Loveless, T.D. Preamble-based RF-DNA Fingerprinting Under Varying Temperatures. 2023 12th Mediterranean Conference on Embedded Computing (MECO). IEEE, 2023, pp. 1–8.
135. Shi, Y.; Davaslioglu, K.; Sagduyu, Y.E. Generative adversarial network for wireless signal spoofing. Proceedings of the ACM Workshop on Wireless Security and Machine Learning, 2019, pp. 55–60.
136. Shi, Y.; Davaslioglu, K.; Sagduyu, Y.E. Generative adversarial network in the air: Deep adversarial learning for wireless signal spoofing. *IEEE Transactions on Cognitive Communications and Networking* **2020**, *7*, 294–303.
137. Restuccia, F.; D'Oro, S.; Al-Shawabka, A.; Rendon, B.C.; Chowdhury, K.; Ioannidis, S.; Melodia, T. Hacking the waveform: Generalized wireless adversarial deep learning. *arXiv preprint arXiv:2005.02270* **2020**.
138. Lalouani, W.; Younis, M.; Baroudi, U. Countering radiometric signature exploitation using adversarial machine learning based protocol switching. *Computer Communications* **2021**, *174*, 109–121.
139. Abanto-Leon, L.F.; Bäuml, A.; Sim, G.H.; Hollick, M.; Asadi, A. Stay connected, leave no trace: Enhancing security and privacy in wifi via obfuscating radiometric fingerprints. *Proceedings of the ACM on Measurement and Analysis of Computing Systems* **2020**, *4*, 1–31.
140. Karunaratne, S.; Krijestorac, E.; Cabric, D. Penetrating RF fingerprinting-based authentication with a generative adversarial attack. ICC 2021-IEEE International Conference on Communications. IEEE, 2021, pp. 1–6.
141. Nikoofard, A.; Givehchian, H.; Bhaskar, N.; Schulman, A.; Bharadia, D.; Mercier, P.P. Protecting Bluetooth User Privacy through Obfuscation of Carrier Frequency Offset. *IEEE Transactions on Circuits and Systems II: Express Briefs* **2022**.
142. Sun, L.; Ke, D.; Wang, X.; Huang, Z.; Huang, K. Robustness of Deep Learning-Based Specific Emitter Identification under Adversarial Attacks. *Remote Sensing* **2022**, *14*, 4996.
143. Ke, D.; Huang, Z.; Wang, X.; Sun, L. Application of adversarial examples in communication modulation classification. 2019 International Conference on Data Mining Workshops (ICDMW). IEEE, 2019, pp. 877–882.
144. Goodfellow, I.J.; Shlens, J.; Szegedy, C. Explaining and harnessing adversarial examples. *arXiv preprint arXiv:1412.6572* **2014**.
145. Madry, A.; Makelov, A.; Schmidt, L.; Tsipras, D.; Vladu, A. Towards deep learning models resistant to adversarial attacks. *arXiv preprint arXiv:1706.06083* **2017**.
146. Carlini, N.; Wagner, D. Towards evaluating the robustness of neural networks. 2017 IEEE symposium on security and privacy (sp). IEEE, 2017, pp. 39–57.
147. Han, H.; Cui, L.; Li, W.; Huang, L.; Cai, Y.; Cai, J.; Zhang, Y. Radio Frequency Fingerprint Based Wireless Transmitter Identification Against Malicious Attacker: An Adversarial Learning Approach. 2020 International Conference on Wireless Communications and Signal Processing (WCSP). IEEE, 2020, pp. 310–315.
148. Defense Advances Research Projects Agency (DARPA). Spectrum Collaboration Challenge — Using AI to Unlock the True Potential of the RF Spectrum. https://archive.darpa.mil/sc2/, 2017.
149. Defense Advances Research Projects Agency (DARPA). Radio Frequency Machine Learning Systems. https://www.darpa.mil/program/radio-frequency-machine-learning-systems, 2019.
150. Yang, Y.; Hu, A.; Yu, J.; Li, G.; Zhang, Z. Radio frequency fingerprint identification based on stream differential constellation trace figures. *Physical Communication* **2021**, *49*, 101458.
151. Tyler, J.H.; Fadul, M.K.; Reising, D.R.; Liang, Y. Assessing the Presence of Intentional Waveform Structure In Preamble-based SEI. GLOBECOM 2022 - 2022 IEEE Global Communications Conference, 2022, pp. 4129–4135. doi:10.1109/GLOBECOM48099.2022.10001025.

152. Al-Shawabka, A.; Restuccia, F.; D'Oro, S.; Jian, T.; Costa Rendon, B.; Soltani, N.; Dy, J.; Ioannidis, S.; Chowdhury, K.; Melodia, T. Exposing the Fingerprint: Dissecting the Impact of the Wireless Channel on Radio Fingerprinting. IEEE INFOCOM 2020 - IEEE Conference on Computer Communications, 2020, pp. 646–655. doi:10.1109/INFOCOM41043.2020.9155259.
153. Hamdaoui, B.; Basha, N.; Sivanesan, K. Deep Learning-Enabled Zero-Touch Device Identification: Mitigating the Impact of Channel Variability Through MIMO Diversity. *IEEE Communications Magazine* **2023**, *61*, 80–85.
154. Downey, J.; Hilburn, B.; O'Shea, T.; West, N. In the Future, AIs—Not Humans—Will Design Our Wireless Signals. *IEEE Spectrum Magazine* **2020**.
155. Tyler, J.H.; Reising, D.R.; Kandah, F.I.; Kaplanoglu, E.; Fadul, M.M.K. Physical Layer-Based IoT Security: An Investigation Into Improving Preamble-Based SEI Performance When Using Multiple Waveform Collections. *IEEE Access* **2022**, *10*, 133601–133616. doi:10.1109/ACCESS.2022.3232463.
156. Li, H.; Gupta, K.; Wang, C.; Ghose, N.; Wang, B. RadioNet: Robust Deep-Learning Based Radio Fingerprinting. 2022 IEEE Conference on Communications and Network Security (CNS), 2022, pp. 190–198. doi:10.1109/CNS56114.2022.9947255.
157. Smith, L.; Smith, N.; Rayborn, D.; Tang, B.; Ball, J.E.; Young, M. Identifying unlabeled WiFi devices with zero-shot learning. Automatic Target Recognition XXX. SPIE, 2020, Vol. 11394, pp. 129–137.
158. Reus-Muns, G.; Jaisinghani, D.; Sankhe, K.; Chowdhury, K.R. Trust in 5G open RANs through machine learning: RF fingerprinting on the POWDER PAWR platform. GLOBECOM 2020-2020 IEEE Global Communications Conference. IEEE, 2020, pp. 1–6.
159. O'shea, T.J.; West, N. Radio machine learning dataset generation with gnu radio. Proceedings of the GNU Radio Conference, 2016, Vol. 1.
160. Sankhe, K.; Belgiovine, M.; Zhou, F.; Riyaz, S.; Ioannidis, S.; Chowdhury, K. ORACLE: Optimized Radio clAssification through Convolutional neuraL nEtworks. IEEE INFOCOM 2019 - IEEE Conference on Computer Communications, 2019, pp. 370–378. doi:10.1109/INFOCOM.2019.8737463.
161. Hanna, S.; Karunaratne, S.; Cabric, D. WiSig: A large-scale WiFi signal dataset for receiver and channel agnostic RF fingerprinting. *IEEE Access* **2022**, *10*, 22808–22818.
162. Jian, T.; Gong, Y.; Zhan, Z.; Shi, R.; Soltani, N.; Wang, Z.; Dy, J.; Chowdhury, K.; Wang, Y.; Ioannidis, S. Radio frequency fingerprinting on the edge. *IEEE Transactions on Mobile Computing* **2021**, *21*, 4078–4093.
163. Zhang, T.; Ye, S.; Zhang, K.; Tang, J.; Wen, W.; Fardad, M.; Wang, Y. A systematic dnn weight pruning framework using alternating direction method of multipliers. Proceedings of the European conference on computer vision (ECCV), 2018, pp. 184–199.
164. He, K.; Zhang, X.; Ren, S.; Sun, J. Deep residual learning for image recognition. Proceedings of the IEEE conference on computer vision and pattern recognition, 2016, pp. 770–778.
165. Lin, D.; Wu, W. RF Fingerprint-Identification-Based Reliable Resource Allocation in an Internet of Battle Things. *IEEE Internet of Things Journal* **2022**, *9*, 21111–21120.
166. Xu, Z.; Han, G.; Liu, L.; Zhu, H.; Peng, J. A Lightweight Specific Emitter Identification Model for IIoT Devices Based on Adaptive Broad Learning. *IEEE Transactions on Industrial Informatics* **2022**, pp. 1–10. doi:10.1109/TII.2022.3206309.
167. Ya, T.; Yun, L.; Haoran, Z.; Zhang, J.; Yu, W.; Guan, G.; Shiwen, M. Large-scale real-world radio signal recognition with deep learning. *Chinese Journal of Aeronautics* **2022**, *35*, 35–48.
168. Zhang, S.; Zhang, Y.; Sun, J.; Gui, G.; Lin, Y.; Gacanin, H.; Adachi, F. A real-world radio frequency signal dataset based on LTE system and variable channels. *arXiv preprint arXiv:2205.12577* **2022**.
169. Zhang, Y.; Peng, Y.; Sun, J.; Gui, G.; Lin, Y.; Mao, S. GPU-Free Specific Emitter Identification Using Signal Feature Embedded Broad Learning. *IEEE Internet of Things Journal* **2023**.
170. Zhang, Y.; Peng, Y.; Adebisi, B.; Gui, G.; Gacanin, H.; Sari, H. Specific Emitter Identification Based on Radio Frequency Fingerprint Using Multi-Scale Network. 2022 IEEE 96th Vehicular Technology Conference (VTC2022-Fall). IEEE, 2022, pp. 1–5.
171. Kuzdeba, S.; Robinson, J.; Carmack, J.; Couto, D. Systems View to Designing RF Fingerprinting for Real-World Operations. Proceedings of the 2022 ACM Workshop on Wireless Security and Machine Learning, 2022, pp. 33–38.
172. Taha, M.A.; Fadul, M.K.; Tyler, J.H.; Reising, D.R.; Loveless, T.D. An assessment of entropy-based data reduction for SEI within IoT applications. MILCOM 2022-2022 IEEE Military Communications Conference (MILCOM). IEEE, 2022, pp. 385–392.

173. Fadul, M.; Reising, D.; Weerasena, L. An Investigation into the Impacts of Deep Learning-based Re-sampling on Specific Emitter Identification Performance. *Authorea Preprints* **2022**.
174. Krug, S.; O'Nils, M. IoT Communication Introduced Limitations for High Sampling Rate Applications. GI/ITG KuVS Fachgespräch Sensornetze–FGSN 2018, 2018.
175. Long, J.D.; Temple, M.A.; Rondeau, C.M. Discriminating WirelessHART Communication Devices Using Sub-Nyquist Stimulated Responses. *Electronics* **2023**, *12*, 1973.
176. Deng, P.; Hong, S.; Qi, J.; Wang, L.; Sun, H. A Lightweight Transformer-Based Approach of Specific Emitter Identification for the Automatic Identification System. *IEEE Transactions on Information Forensics and Security* **2023**.
177. Vaswani, A.; Shazeer, N.; Parmar, N.; Uszkoreit, J.; Jones, L.; Gomez, A.N.; Kaiser, Ł.; Polosukhin, I. Attention is all you need. *Advances in neural information processing systems* **2017**, *30*.
178. Shen, G.; Zhang, J.; Marshall, A.; Woods, R.; Cavallaro, J.; Chen, L. Towards Receiver-Agnostic and Collaborative Radio Frequency Fingerprint Identification. *arXiv preprint arXiv:2207.02999* **2022**.
179. Qian, Y.; Qi, J.; Kuai, X.; Han, G.; Sun, H.; Hong, S. Specific emitter identification based on multi-level sparse representation in automatic identification system. *IEEE Transactions on Information Forensics and Security* **2021**, *16*, 2872–2884.
180. Liu, Z.; Lin, Y.; Cao, Y.; Hu, H.; Wei, Y.; Zhang, Z.; Lin, S.; Guo, B. Swin transformer: Hierarchical vision transformer using shifted windows. Proceedings of the IEEE/CVF international conference on computer vision, 2021, pp. 10012–10022.
181. Wu, H.; Xiao, B.; Codella, N.; Liu, M.; Dai, X.; Yuan, L.; Zhang, L. Cvt: Introducing convolutions to vision transformers. Proceedings of the IEEE/CVF International Conference on Computer Vision, 2021, pp. 22–31.
182. Nguyen, D.D.N.; Sood, K.; Xiang, Y.; Gao, L.; Chi, L.; Yu, S. Towards IoT Node Authentication Mechanism in Next Generation Networks. *IEEE Internet of Things Journal* **2023**.
183. Merchant, K.; Nousain, B. Toward receiver-agnostic RF fingerprint verification. 2019 IEEE Globecom Workshops (GC Wkshps). IEEE, 2019, pp. 1–6.
184. He, B.; Wang, F. Cooperative specific emitter identification via multiple distorted receivers. *IEEE Transactions on Information Forensics and Security* **2020**, *15*, 3791–3806.
185. Huang, K.; Jiang, B.; Yang, J.; Wang, J.; Hu, P.; Li, Y.; Shao, K.; Zhao, D. Cross-receiver specific emitter identification based on a deep adversarial neural network with separated batch normalization. Third International Conference on Computer Science and Communication Technology (ICCSCT 2022). SPIE, 2022, Vol. 12506, pp. 1659–1663.
186. Zhao, T.; Sarkar, S.; Krijestorac, E.; Cabric, D. GAN-RXA: A Practical Scalable Solution to Receiver-Agnostic Transmitter Fingerprinting. *arXiv preprint arXiv:2303.14312* **2023**.
187. Zha, X.; Li, T.; Qiu, Z.; Li, F. Cross-Receiver Radio Frequency Fingerprint Identification Based on Contrastive Learning and Subdomain Adaptation. *IEEE Signal Processing Letters* **2023**, *30*, 70–74.
188. Tatarek, T.; Kronenberger, J.; Handmann, U. Functionality, advantages and limits of the tesla autopilot **2017**.
189. Soori, M.; Arezoo, B.; Dastres, R. Artificial Intelligence, Machine Learning and Deep Learning in Advanced Robotics, A Review. *Cognitive Robotics* **2023**.
190. Shen, G.; Zhang, J.; Marshall, A.; Cavallaro, J.R. Towards scalable and channel-robust radio frequency fingerprint identification for LoRa. *IEEE Transactions on Information Forensics and Security* **2022**, *17*, 774–787.
191. Chen, X.; He, K. Exploring simple siamese representation learning. Proceedings of the IEEE/CVF conference on computer vision and pattern recognition, 2021, pp. 15750–15758.
192. Zhu, Y.; Zhuang, F.; Wang, J.; Ke, G.; Chen, J.; Bian, J.; Xiong, H.; He, Q. Deep subdomain adaptation network for image classification. *IEEE transactions on neural networks and learning systems* **2020**, *32*, 1713–1722.
193. Ma, H.; Qiu, H.; Gao, Y.; Zhang, Z.; Abuadbba, A.; Fu, A.; Al-Sarawi, S.; Abbott, D. Quantization backdoors to deep learning models. *arXiv preprint arXiv:2108.09187* **2021**.
194. Capotondi, A.; Rusci, M.; Fariselli, M.; Benini, L. CMix-NN: Mixed low-precision CNN library for memory-constrained edge devices. *IEEE Transactions on Circuits and Systems II: Express Briefs* **2020**, *67*, 871–875.
195. Alom, M.Z.; Moody, A.T.; Maruyama, N.; Van Essen, B.C.; Taha, T.M. Effective quantization approaches for recurrent neural networks. 2018 international joint conference on neural networks (IJCNN). IEEE, 2018, pp. 1–8.

196. Tyler, J.; Fadul, M.; Hilling, M.; Reising, D.; Loveless, D. Assessing Adversarial Replay and Deep Learning-Driven Attacks on Specific Emitter Identification-based Security Approaches. *IEEE Open Journal of the Communications Society (Accepted)* **2023**.
197. Kaushal, N.; Kaushal, P. Human identification and fingerprints: a review. *J biomet biostat* **2011**, *2*, 2.
198. Henke, C. A Comprehensive Guide to IoT Protocols. *emnify* **2022**.

Disclaimer/Publisher's Note: The statements, opinions and data contained in all publications are solely those of the individual author(s) and contributor(s) and not of MDPI and/or the editor(s). MDPI and/or the editor(s) disclaim responsibility for any injury to people or property resulting from any ideas, methods, instructions or products referred to in the content.